
Masters Theses

Student Theses and Dissertations

Spring 2011

Design of a conditioner for smoothing wind turbine output power

Murali Bottu

Follow this and additional works at: https://scholarsmine.mst.edu/masters_theses



Part of the [Electrical and Computer Engineering Commons](#)

Department:

Recommended Citation

Bottu, Murali, "Design of a conditioner for smoothing wind turbine output power" (2011). *Masters Theses*. 4900.

https://scholarsmine.mst.edu/masters_theses/4900

This thesis is brought to you by Scholars' Mine, a service of the Missouri S&T Library and Learning Resources. This work is protected by U. S. Copyright Law. Unauthorized use including reproduction for redistribution requires the permission of the copyright holder. For more information, please contact scholarsmine@mst.edu.

DESIGN OF A CONDITIONER FOR SMOOTHING WIND TURBINE OUTPUT
POWER

by

MURALI BOTTU

A THESIS

Presented to the Faculty of the Graduate School of the
MISSOURI UNIVERSITY OF SCIENCE AND TECHNOLOGY

In Partial Fulfillment of the Requirements for the Degree
MASTER OF SCIENCE IN ELECTRICAL ENGINEERING

2011

Approved by

Dr. Mariesa L. Crow, Advisor
Dr. Badrul H. Chowdhury
Dr. Mehdi Ferdowsi

© 2011

Murali Bottu

All Rights Reserved

ABSTRACT

As a result of wind speed intermittency, wind turbine output power can be highly variable. The large variability in output power can adversely impact local loads that are sensitive to pulsating power. To mitigate large swings in power, the wind turbine output power can be smoothed by using a small energy buffer. A power conditioner is proposed to smooth the wind power output by utilizing the energy of an ultracapacitor. The conditioner is based on a single phase voltage source inverter (VSI) connected between the grid interconnection point and the ultracapacitor. The shunt VSI injects or absorbs active power from the line to smooth the wind power output by utilizing the short term storage capabilities of the ultracapacitor. The ultracapacitor is connected to the DC link through a DC-DC converter. The bidirectional DC-DC converter acts in buck mode during discharge and in boost mode during charging to maintain the voltage of the DC link relatively constant to provide good controllability of the VSI. The control strategies for the conditioner are presented in this thesis. The simulation results show that the power quality conditioner is efficient in smoothing the wind power. To understand how effectively the power conditioner smoothes the wind turbine output in real time operational conditions, a hardware prototype for verification is developed in addition to software simulation. The bidirectional DC-DC converter and VSI are constructed and tested in the laboratory and then field tested. The control of the bidirectional DC-DC converter is implemented using the microchip PIC24FJ128GA010 microcontroller. The gate signals for the IGBTs in the VSI are obtained from the TI TMDSDOCK28335 digital signal controller. The conditioner design and control are validated on a Skystream 3.7 wind turbine installed at Missouri University of Science & Technology.

ACKNOWLEDGMENTS

I would like to express my sincere gratitude to my advisor, Dr. Mariesa Crow, for her guidance, supervision and encouragement throughout my Master's program and with my research. She has been a continuous source of motivation and has helped me to develop my skills. I dedicate this thesis to her.

I would like to thank Dr. Mehdi Ferdowsi and Dr. Badrul Chowdhury for their time and effort in serving as committee members and helping through my graduate studies. I would like to thank Mr. Jerry L. Tichenor and Dr. Jonathan Kimball, who have been very helpful throughout my work.

Lastly, I am obliged to my parents, my sister, and my friends who have been very supportive throughout my studies offering encouragement. Without their support, I would not have been achieved my Master's study.

TABLE OF CONTENTS

	Page
ABSTRACT.....	iii
ACKNOWLEDGMENTS	iv
TABLE OF CONTENTS.....	v
LIST OF ILLUSTRATIONS.....	vii
LIST OF TABLES	ix
NOMENCLATURE	x
SECTION	
1. INTRODUCTION.....	1
1.1 MOTIVATION.....	1
1.2 PROPOSED APPROACH.....	1
1.3 CONTRIBUTIONS OF THE THESIS.....	2
1.4 OUTLINE OF THESIS.....	3
2. WIND TURBINE AND ULTRACAPACITOR	5
2.1 INSTALLED WIND TURBINE	5
2.2 SIMULINK MODEL OF THE WIND TURBINE.....	7
2.3 SIMULATION RESULTS	7
2.4 ULTRACAPACITOR ELECTRIC CIRCUIT MODEL	8
3. POWER QUALITY CONDITIONER.....	11
3.1 POWER CONDITIONER TOPOLOGY.....	11
3.2 EQUIVALENT CIRCUIT OF THE CONDITIONER.....	12
3.3 CONSTRUCTION OF THE POWER QUALITY CONDITIONER.....	14
4. BIDIRECTIONAL DC-DC CONVERTER.....	16
4.1 DC-DC CONVERTER TOPOLOGY	16
4.2 CONTROL OF THE DC-DC CONVERTER	17
4.3 SIMULATION RESULTS	20
4.4 CONSTRUCTION OF THE DC-DC CONVERTER	20
4.4.1 PIC Microcontroller	22

4.4.2 Voltage Measuring Circuit	24
4.4.3 Gate Driver Circuit	26
4.5 HARDWARE RESULTS	27
5. SHUNT INVERTER	30
5.1 TOPOLOGY OF THE VSI	30
5.2 CONTROL OF THE SHUNT INVERTER	31
5.3 CONSTRUCTION OF THE SINGLE PHASE VSI	33
5.3.1 Measurement Circuit	33
5.3.2 Signal Shaping Circuit	33
5.3.3 Digital Signal Controller	34
5.3.4 PWM Signal Generation	37
5.4 HARDWARE RESULTS	37
6. SYSTEM VALIDATION	42
6.1 SIMULATION RESULTS	42
6.2 HARDWARE RESULTS	45
7. CONCLUSION AND FUTURE WORK	49
APPENDIX: LIST OF THE COMPONENTS	50
BIBLIOGRAPHY	52
VITA	54

LIST OF ILLUSTRATIONS

Figure	Page
2.1. Wind Turbine Installed at the Missouri University of Science and Technology.....	5
2.2. The Actual Output Power of Installed Wind Turbine (blue) and the Target Smoothed Power (red).....	6
2.3. Skystream3.7 Wind Turbine Connections to the Grid.....	7
2.4. Modeled Active Power Output of the Wind Turbine.....	8
2.5. Electric Model of the Ultracapacitor.....	9
3.1. Topology of the Power Quality Conditioner	12
3.2. Equivalent Circuit of the Conditioner.....	13
3.3. Power Quality Conditioner Architecture	15
4.1. Bidirectional DC-DC Converter	17
4.2. Flowchart Showing the Control Strategy of the Bidirectional DC-DC Converter ...	18
4.3. DC-DC Converter Controller.....	19
4.4. Voltage of the Ultracapacitor and the DC Link.....	20
4.5. Flowchart Showing the Construction of the DC-DC Converter.....	21
4.6. Flowchart Showing the Operation of the Microcontroller.....	23
4.7. Voltage Measuring Circuit.....	25
4.8. Gate Driver Circuit	26
4.9. Experimental Setup of the Bidirectional DC-DC Converter	27
4.10. Gate Signals in Buck Mode and Boost Mode.....	28
4.11. Gate Signals from Driver in Buck Mode and in Boost Mode	28
4.12. Voltage of the DC Link.....	29
4.13. Voltage of the Ultracapacitor.....	29
5.1. Circuit Diagram of the Shunt Inverter	31
5.2. Shunt Inverter Control Scheme.....	32
5.3. Signal Shaping Circuit using Operational Amplifier.....	33
5.4. Voltage Regulation Circuit using LM317.....	34
5.5. Signal Shaping Circuit Input and Output.....	34
5.6. DSP Main Loop Program Structure.....	35

5.7. Test Results of the ADC Converter 1 and 2 in the Module	36
5.8. Test Result of the Low Pass Filter	37
5.9. Gate Signals from the DSP and Dead Time Implemented	38
5.10. Gate Signals from the Driver and Dead Time Implemented	38
5.11. Experimental Setup of the Single Phase VSI.....	39
5.12. Output Voltage of the Inverter without Filter	40
5.13. Output Voltage of the Inverter with RL Filter	41
5.14. Output Current of the Inverter with RL Filter	41
5.15. Output Voltage of the Inverter with LC Filter	41
6.1. Modeled Active Power Output of the Wind Turbine.....	43
6.2. Reference Power Obtained from the Low Pass Filter.....	43
6.3. Active Power Output of the Wind Turbine Model	44
6.4. Conditioner Active Power.....	44
6.5. Smoothed Power at the Grid Interconnection Point	44
6.6. Experimental Setup of the Power Quality Conditioner	45
6.7. Power Quality Conditioner Connections to the Wind Turbine Output.....	46
6.8. Measured RMS Voltage at the Output of the Wind Turbine	46
6.9. RMS Current Measured at the Output of the Wind Turbine	47
6.10. Measured RMS Current after connecting the Conditioner	48
6.11. Ultracapacitor RMS Voltage.....	48

LIST OF TABLES

Table	Page
4.1. Ultracapacitor Voltage Measurements.....	25
4.2. DC Link Voltage Measurements	26
6.1. Simulation Parameters	42

NOMENCLATURE

Symbol	Description
ESR	Equivalent Series Resistor
VSI	Voltage Source Inverter
E_{cap}	Energy Stored in the Ultracapacitor
V_i	Initial Voltage
V_f	Final Voltage
P_{wind}	Active Power of the Wind Turbine
P_{ucap}	Active Power Supplied by the Ultracapacitor
P_{grid}	Active Power at the Grid Interconnection Point
P_{ref}	Reference Power
T	Time Constant of the Filter

1. INTRODUCTION

1.1 MOTIVATION

Due to the price volatility and carbon impact of fossil fuels, wind power generation is rapidly growing as an alternative energy source in many parts of the world. Due to the intermittency of wind speed, wind turbine output power can be highly variable. Power fluctuations from the wind turbine may cause severe power quality problems when connected to a weak grid, such as a residential network or microgrid. The large variability in wind turbine output power can adversely impact local loads that are sensitive to pulsating power, posing a challenge to the use of wind power extensively. The rapid growth of the wind power and its immense potential as a future energy source encourages us to find a way to smooth the intermittent wind power. Energy storage technologies can be used to improve the quality of the wind power [1], [2].

1.2 PROPOSED APPROACH

In this thesis, the power quality conditioner with the ultracapacitor is proposed to smooth the variable wind turbine output power. The short term storage capabilities of the ultracapacitor can be effectively used to smooth the variable wind power to minimize rapid power excursions that may damage sensitive local loads. This thesis presents a power conditioner that has the purpose of smoothing the wind turbine output power. The power conditioner mainly consists of power converters to shape the injected current at the point of common coupling [3]. Power electronic controllers have large applications in power systems. The conditioner is based on a single phase shunt connected VSI connected between the grid interconnection point and the DC link. The shunt VSI injects or absorbs active power from the line to smooth the intermittent wind power by charging or discharging the ultracapacitor [4]. The ultracapacitor is connected to the DC link through a DC-DC converter. Traditionally, the VSI DC link voltage is maintained relatively constant by the shunt inverter control [5]-[7]. In this application, a bidirectional DC-DC converter is used to maintain the DC link voltage relatively constant [8]. The bidirectional DC-DC converter acts in buck mode during discharge of the DC link and in

boost mode during charging the DC link to maintain the voltage of the DC link relatively constant to provide good controllability of the VSI. The conditioner works modifying the power flow at the grid interconnection point.

Control of the injected active power via the shunt inverter is presented in this thesis. The VSI controller calculates the compensating active power, which is then synthesized by using the pulse width modulation (PWM) switching sequence. The reference signal to the shunt inverter controller is obtained from a low pass filter, which has a large time constant. The smoothing performance of the conditioner depends on the time constant of the low pass filter. The fluctuating wind power is passed through the low pass filter to get the smoothed reference value. The conditioner ensures the smooth power is available at the grid interconnection point. The simulation results are presented to show the efficiency of the conditioner in smoothing the variable wind turbine output power.

The bidirectional DC-DC converter is constructed and tested in the laboratory. The gate signals for the converter are obtained from the microchip PIC128FJ128GA010 microcontroller. The single phase VSI is also constructed and tested in the laboratory. The gate signals for the IGBTs in the VSI are obtained from the TI TMDSDOCK28335 digital signal controller. The measurement board, signal shaping board and gate driver boards are constructed and tested in the laboratory. The inverter is connected to the output line through the filter to reduce the noise. The power conditioner design and control is further validated on the Skystream3.7 wind turbine installed at the Missouri University of Science and Technology.

1.3 CONTRIBUTIONS OF THE THESIS

The main contributions of this thesis are:

- development of the power quality conditioner design with an ultracapacitor for smoothing the pulsating wind power,
- development of the bidirectional DC-DC converter and the shunt inverter topologies used in the conditioner,
- development of the control schemes for the bidirectional DC-DC converter and the shunt inverter,

- presenting the simulation results to show the conditioner is efficient in smoothing the wind power,
- construction and implementation of the power quality conditioner to smooth the wind turbine output power,
- implementation of the control strategies of the conditioner by the microcontroller and digital signal controller, and
- validation of the hardware results.

1.4 OUTLINE OF THESIS

The thesis is composed of seven sections. Section 1 provides a general introduction and limitations for the use of wind energy extensively. The conditioner is proposed to smooth the output power of the wind turbine.

Section 2 describes the installed wind turbine output power and target power to be achieved. The simulink model of the wind turbine is described and its results are presented. The ultracapacitor model is described in this section.

Section 3 presents the topology of the power quality conditioner to smooth the variable power of the wind turbine. The equivalent circuit of the conditioner and the overview of the power quality conditioner hardware architecture are described in this section.

Section 4 describes the topology of the bi-directional DC-DC converter and its control to maintain the voltage of the DC link at reference value. The hardware implementation and testing of the bi-directional DC-DC converter is described in this section. This section describes the PIC microcontroller operation in the control of the DC-DC converter. The measurement circuits and gate driver circuits are described in this section. The simulation and hardware results of the DC-DC converter with ultracapacitor are presented in this section.

Section 5 describes the topology of the shunt connected voltage source inverter and its control. The hardware construction and testing of the shunt inverter is described in this section. The measurement circuits, signal conditioning circuit and the gate driver

circuits are described in this section. The simulation and hardware results of the converter are presented in this section. This section describes the filter at the output of the inverter.

Section 6 presents the system validation after connecting the conditioner to the wind turbine. The results are presented in this section to show that conditioner is efficient in smoothing variable wind turbine power.

Section 7 presents the conclusions and the main contributions of this thesis. Suggestions for future research work are also presented.

2. WIND TURBINE AND ULTRACAPACITOR

2.1 INSTALLED WIND TURBINE

The Skystream3.7 wind turbine shown in Figure 2.1 is installed at the Missouri University of Science and Technology. The actual (measured) output power of the Skystream3.7 wind turbine is shown in Figure 2.2. The wind turbine is connected to the campus grid. The line to line voltage and line current are measured using the LEM voltage and current sensors at the output of the wind turbine. These measured analog values are fed to a National Instruments data acquisition module, NI USB-6009, which sends the data to a computer through a USB port. The blue curve represents the actual output power of the wind turbine and the red curve represents the smoothed target power to be obtained after the conditioner is connected to the wind turbine.



Figure 2.1. Wind Turbine Installed at the Missouri University of Science and Technology

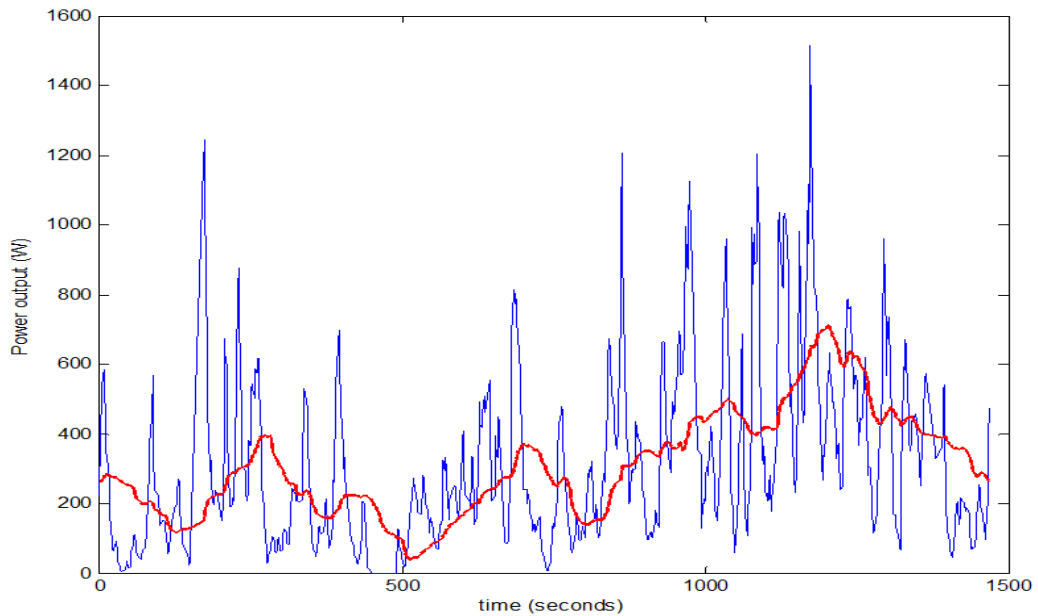


Figure 2.2. The Actual Output Power of Installed Wind Turbine (blue) and the Target Smoothed Power (red)

The Skystream3.7 wind turbine output lines are connected to the campus grid as shown in the Figure 2.3. The neutral and ground terminals of the wind turbine are tied together and connected to the neutral of the grid. The two lines from the wind turbine are connected across one leg of the grid as shown in the Figure 2.3. The power quality conditioner is connected in shunt between the output of the wind turbine and the grid interconnection point.

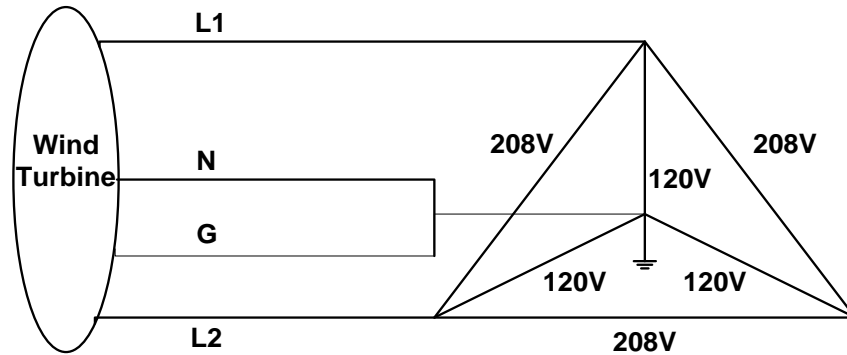


Figure 2.3. Skystream3.7 Wind Turbine Connections to the Grid

2.2 SIMULINK MODEL OF THE WIND TURBINE

The electric model of the variable wind power is designed in MATLAB SIMULINK. This model generates a constant voltage and a randomly variable current, similar to the characteristics of the wind turbine output power. To obtain this model, the variable current is injected in series with the constant voltage source. The power generated by this model is similar to the actual power of the installed wind turbine. This model acts as a variable wind turbine output power source for the simulation, to which the conditioner is connected and its performance is evaluated.

2.3 SIMULATION RESULTS

The variable output power of the wind turbine model developed is shown in Figure 2.4. This model was developed to mimic the actual wind turbine active power output shown in Figure 2.2.

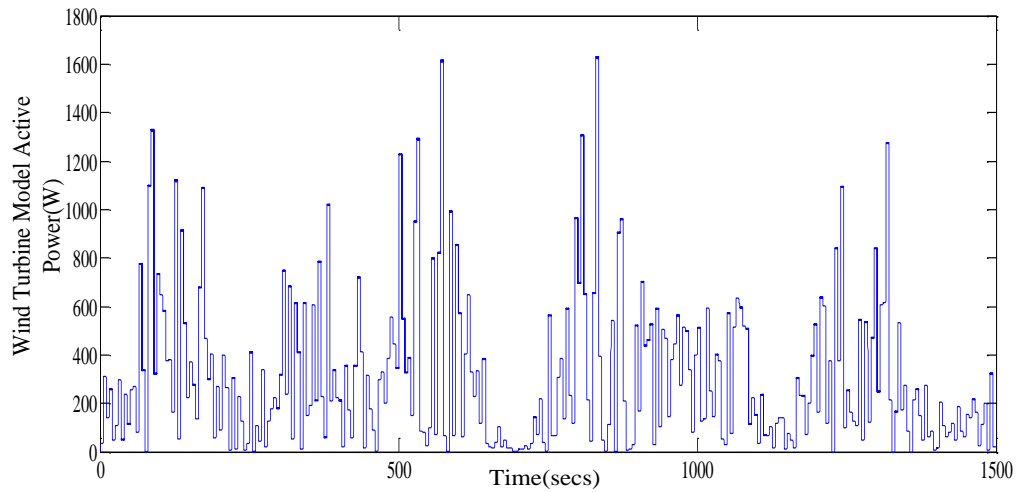


Figure 2.4. Modeled Active Power Output of the Wind Turbine

2.4 ULTRACAPACITOR ELECTRIC CIRCUIT MODEL

Ultracapacitors are double layered, which increases the storage capability by increasing the surface through a porous electrolyte. Ultracapacitors are mainly used in high peak power situations to improve the reliability of electric power systems. Ultracapacitors are electrochemical double layer capacitors that have unique characteristics when compared to other energy storage devices. The high performance characteristics of Maxwell Technologies Ultracapacitors allow developing hybrid power system solutions that cost less and perform better. Ultracapacitors have high energy density and large time constants as well. In the charging mode, the terminal voltage of the ultracapacitor increases, whereas in the discharging mode the terminal voltage of the ultracapacitor is decreased. The simple ultracapacitor model shown in Figure 2.5 contains only one RC branch, which is composed of an equivalent series resistor (ESR) and a capacitor (C) [9]. The ESR represents the ohmic losses in the ultracapacitor. This ultracapacitor model is used in the converter simulation.

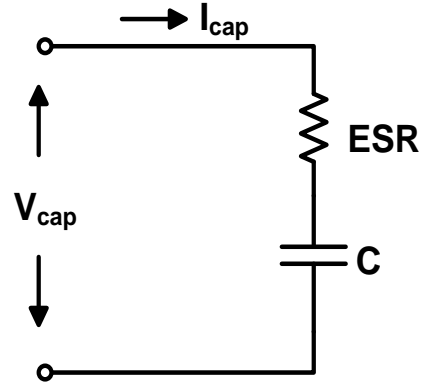


Figure 2.5. Electric Model of the Ultracapacitor

The amount of energy drawn or released by the ultracapacitor is directly proportional to the capacitance value and change in the value of terminal voltage and is given by

$$E_{cap} = \frac{1}{2}c(V_i^2 - V_f^2) \quad (1)$$

where V_i is the initial voltage before charging or discharging starts, and V_f is the final voltage after charging or discharging ends.

The state of charge of the module is directly proportional to the voltage and the capacitance of the module

$$E_{cap} = \frac{1}{2}CV^2 \quad (2)$$

The benefits of using ultracapacitor technology are quite extensive. Ultracapacitors have low losses while charging and discharging. Ultracapacitors have a very low ESR, allowing them to deliver and absorb very high current and to be charged very quickly, making them well suited for energy buffer applications. Ultracapacitors are

highly efficient components, even at very high currents. The characteristics of the ultracapacitor allow it to be charged and discharged at the same rates, something most batteries cannot tolerate. Ultracapacitors have a wide voltage window. The energy storage mechanism of an ultracapacitor is a highly reversible process. The process moves charge and ions only. It does not make or break chemical bonds like batteries; therefore it is capable of millions of cycles with minimal change in performance. The lifetime of the module depends on the capacitance and ESR. It is therefore capable of many years of continuous duty with minimal change in performance. Ultracapacitors makes system integration relatively easy compared to batteries. With all the above features, ultracapacitors are ideally suited for pulse power applications.

3. POWER QUALITY CONDITIONER

3.1 POWER CONDITIONER TOPOLOGY

As shown in Figure 3.1, the power quality conditioner consists of a shunt inverter and a bidirectional DC-DC converter. The VSI acts as a shunt active filter compensating the active power of the wind turbine. The VSI is connected to the line through an RL filter which reduces the unwanted harmonics. The shape of the output current of the conditioner depends on the inductor value of the filter. The value of the resistor and the inductor determines the damping in the circuit. On the other side, the VSI is connected to the DC link capacitor. The DC-DC converter with the ultracapacitor is used to reduce the size of the DC link capacitor and to maintain the voltage of the DC link relatively constant as the ultracapacitor discharges and charges. The bidirectional DC-DC converter charges the ultracapacitor in buck mode by reducing the voltage of the DC link. In the other direction, it acts in boost mode, discharging the ultracapacitor to increase the voltage of the DC link. The power conditioner injects or absorbs active power from the line through the filter to smooth the variable wind turbine output power. The DC link acts as the voltage source for the VSI.

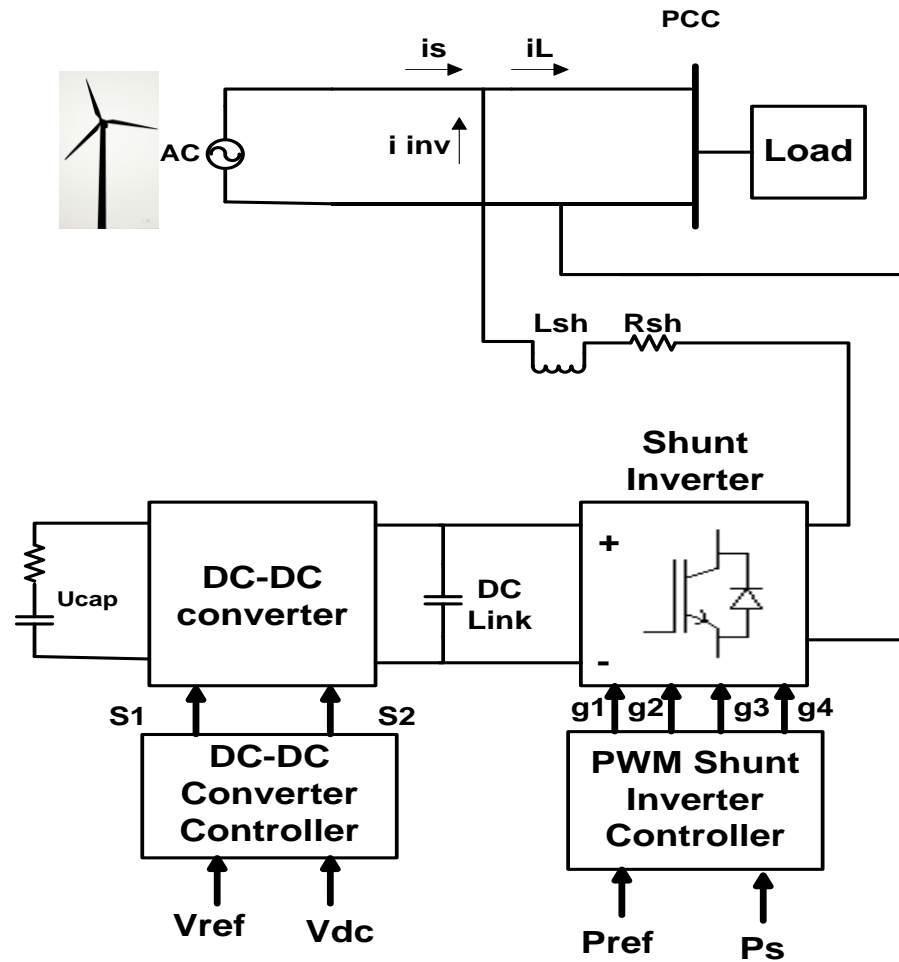


Figure 3.1. Topology of the Power Quality Conditioner

3.2 EQUIVALENT CIRCUIT OF THE CONDITIONER

The wind turbine generator produces a constant voltage and variable current output. Figure 3.2 shows the equivalent circuit of the power conditioner when integrated to the wind turbine, where V_s is the voltage of the wind turbine generator, i_s is the wind turbine current, i_{inv} is the compensating current supplied by the VSI that can be injected

or drawn from the line, and i_L is the smoothed current. The current flow in the system is expressed as

$$i_L(t) = i_s(t) + i_{inv}(t) \quad (3)$$

The relationship between the grid power, wind power and the power from ultracapacitor is given by

$$P_{wind} \pm P_{ucap} = P_{grid} \quad (4)$$

where P_{wind} is the active power of the wind turbine, P_{ucap} is the active power supplied by the ultracapacitor, and P_{grid} is the active power at the grid interconnection point.

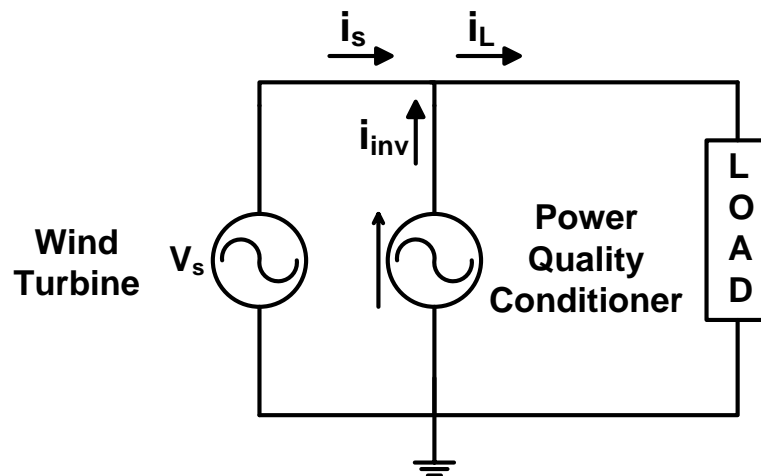


Figure 3.2. Equivalent Circuit of the Conditioner

3.3 CONSTRUCTION OF THE POWER QUALITY CONDITIONER

The power quality conditioner hardware architecture is shown in Figure 3.3. The conditioner is connected at the output of the wind turbine to smooth the pulsating power. It has a single phase VSI, which is capable of injecting or drawing active power from the line. The line current and voltage are measured using the current and voltage sensors on the measurement board. The output of the measurement board is passed through a signal shaping board before passing to a digital signal controller. The sinusoidal PWM signals from the digital signal controller are given to the gate driver circuit. These gate drivers provide the switching signals to the IGBTs. The other side of the inverter is connected to the DC link. The voltage of the DC link is maintained at a near constant value with the bidirectional DC-DC converter and the ultracapacitor. The voltage of the DC link and the ultracapacitor are measured using the LEM voltage sensors on the measurement board. The output signals of the measurement board are sent to the PIC microcontroller. The gate signals from the microcontroller are given to the gate driver circuit. The gate driver circuit board will drive the MOSFETs. The construction of the DC-DC converter and the inverter are discussed in detail in the later sections. The DC-DC converter and the shunt inverter are integrated in the construction of the power conditioner.

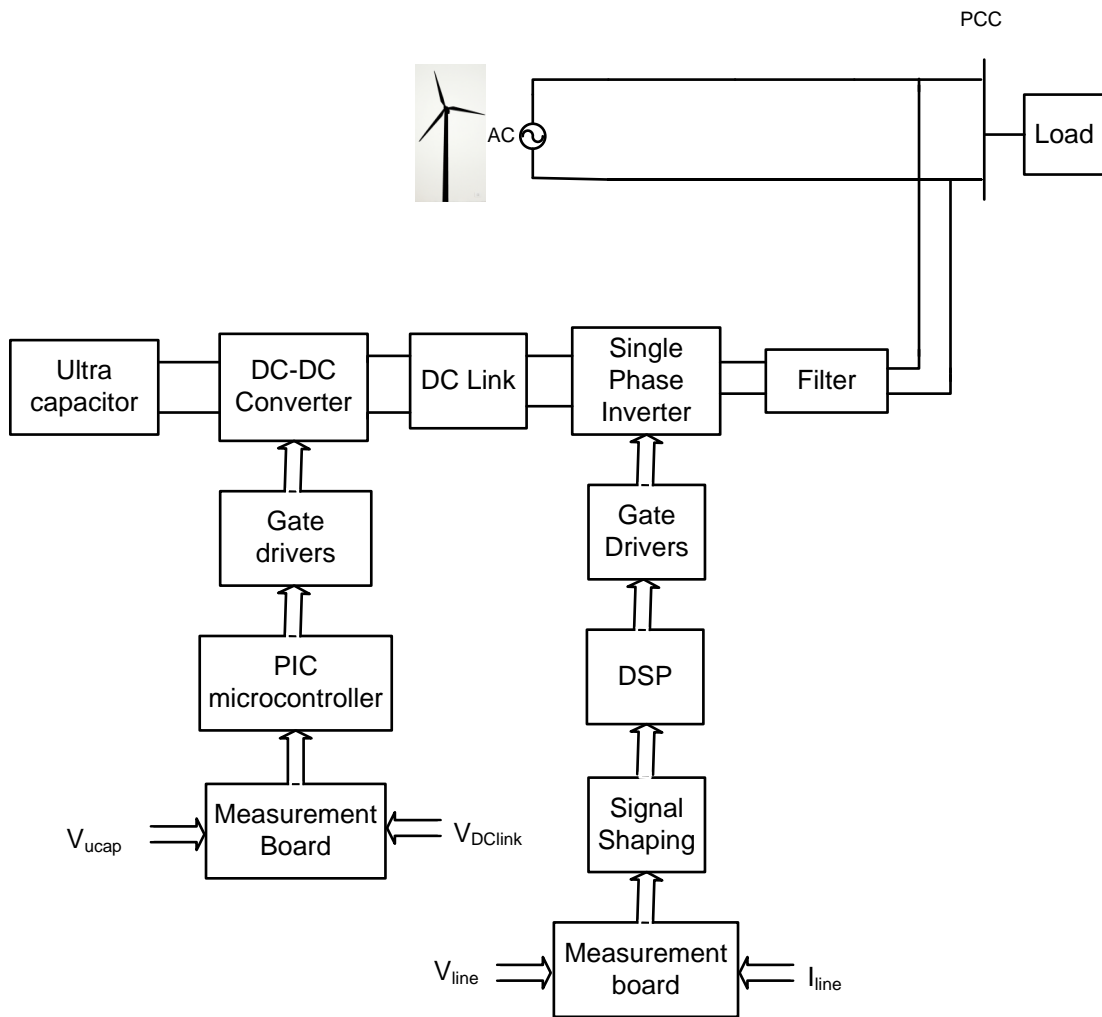


Figure 3.3. Power Quality Conditioner Architecture

4. BIDIRECTIONAL DC-DC CONVERTER

4.1 DC-DC CONVERTER TOPOLOGY

The topology of the bidirectional DC-DC converter is shown in Figure 4.1. The bidirectional DC-DC converter acts a buck converter in one direction and as a boost converter in the other direction [10]-[13]. Power MOSFETS are used as the switching devices in the circuit. The operation of the converter is controlled by the DC link voltage and the voltage of the ultracapacitor. The main purpose of the bidirectional DC-DC converter is to maintain the voltage of the DC link relatively constant at a reference value.

The DC-DC converter operating modes can be divided into four modes as follows:

- Mode 1: The DC-DC converter acts in buck mode, when the voltage of the DC link is above the reference value. In this mode, the DC-DC converter allows the power flow to charge the ultracapacitor.
- Mode 2: The DC-DC converter acts in boost mode, when the voltage of the DC link falls below the reference value. In this mode, the ultracapacitor energy is discharged to increase the voltage of the DC link.
- Mode 3: When the ultracapacitor is fully charged, the DC-DC converter shuts down to avoid damaging the ultracapacitor and the equipment.
- Mode 4: When the ultracapacitor is fully discharged, the conditioner shuts down until charging of the ultracapacitor may resume.

The DC link capacitor is used as an intermediate element between the DC-DC converter and the inverter. The DC link model is:

$$C \frac{dV}{dt} = I_{dc(DC-DC Conv)} - I_{dc(Inv)} \quad (5)$$

where C is the DC link capacitance, $I_{dc(DC-DC Conv)}$ is the current from the DC-DC converter, and $I_{dc(Inv)}$ is the inverter current at the source side.

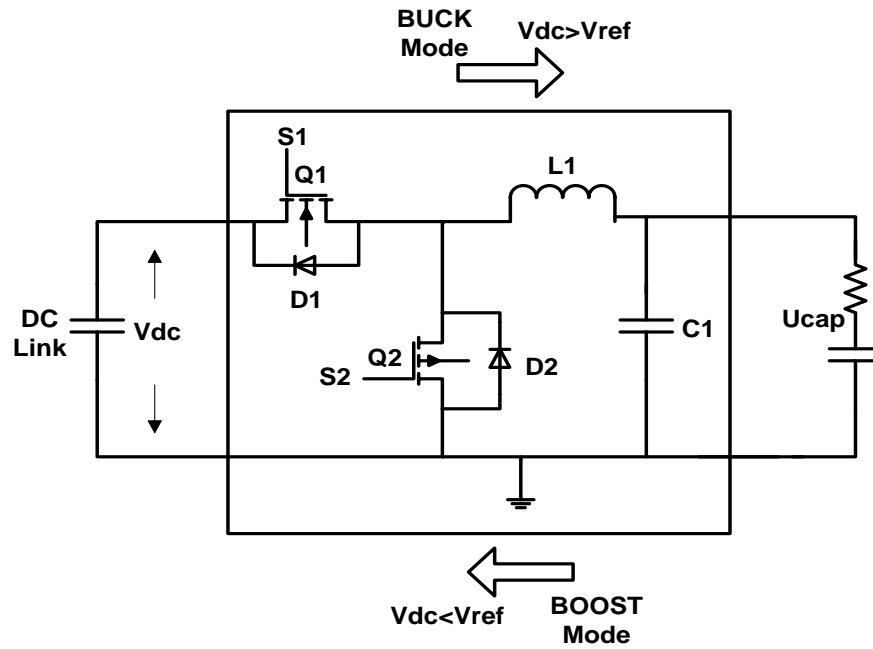


Figure 4.1. Bidirectional DC-DC Converter

4.2 CONTROL OF THE DC-DC CONVERTER

The main objective of the DC-DC controller is to maintain the voltage of the DC link relatively constant at the reference value. The control strategy of the converter is shown in Figure 4.2.

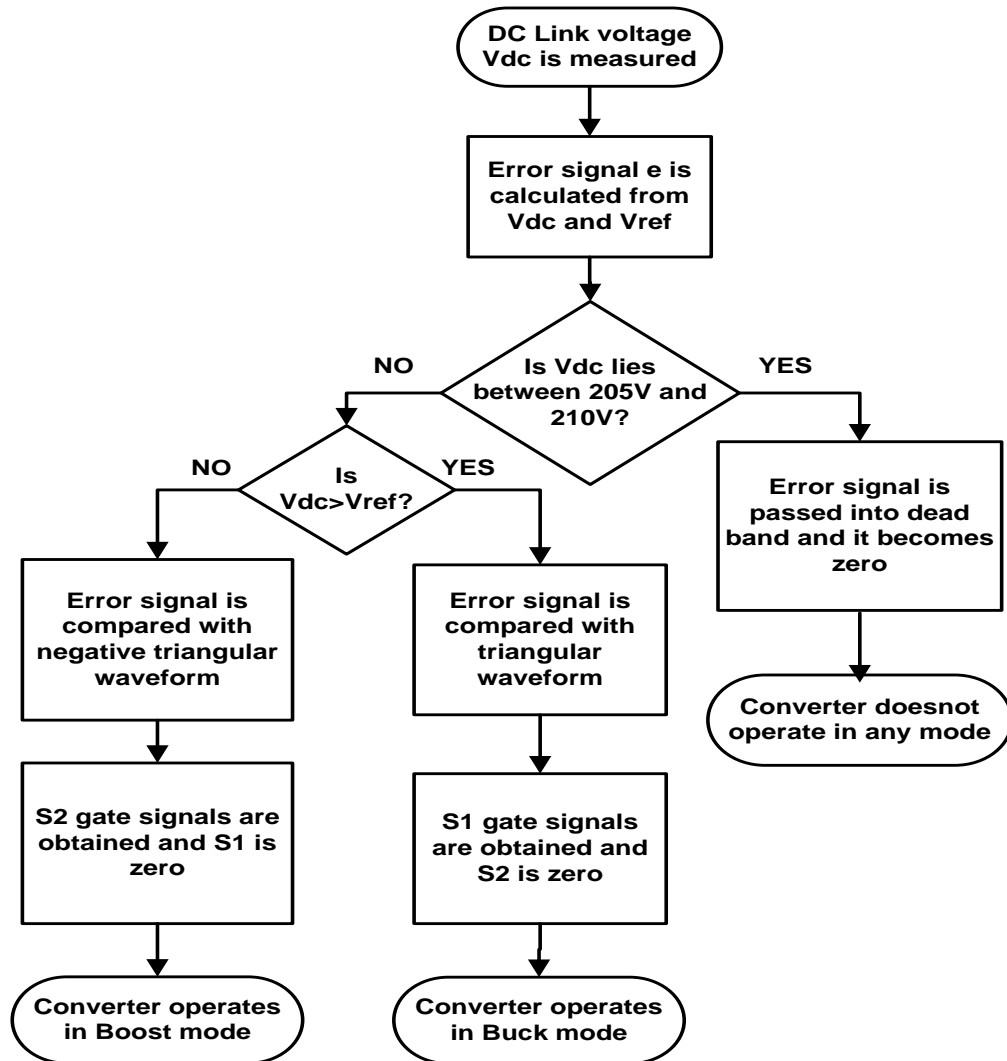


Figure 4.2. Flowchart Showing the Control Strategy of the Bidirectional DC-DC Converter

The DC link voltage is the input for the converter controller. The reference voltage of the DC link is set at 208V. The DC link voltage is subtracted from the reference voltage to obtain the error signal. The generated error signal is passed through a dead band to avoid the unnecessary continuous transfer of the energy in the converter. Then the signal is passed through a PI controller before it is given to the comparator.

Whenever the voltage of the DC link rises above the reference value, the gating signal s_1 is given to the MOSFET Q1 and Q2 is turned off. In this case, the DC-DC converter acts in buck mode reducing the DC link voltage. Whenever, the DC link voltage falls below the reference value, and then gating signal S_2 is given to MOSFET Q2 and Q1 is turned off. In this case, the DC-DC converter acts in boost mode, increasing the DC link voltage. Anti-parallel diodes conduct when the respective switching device is not conducting. Finally, gating signals are selected for MOSFETs between the comparator output and zero, depending on the voltage of the DC link.

The switching sequence of the MOSFETS in the DC-DC converter is as follows.

- If $V_{Dlink} > V_{ref}$, then Q1 operates with duty cycle obtained from the comparator and Q2 is turned off.
- If $V_{Dlink} < V_{ref}$, then Q2 operates with duty cycle obtained from the comparator and Q1 is turned off.

The controller for the bidirectional DC-DC converter designed in the MATLAB is shown in Figure 4.3. The gating signals thus obtained are given to the MOSFETs in the converter circuit.

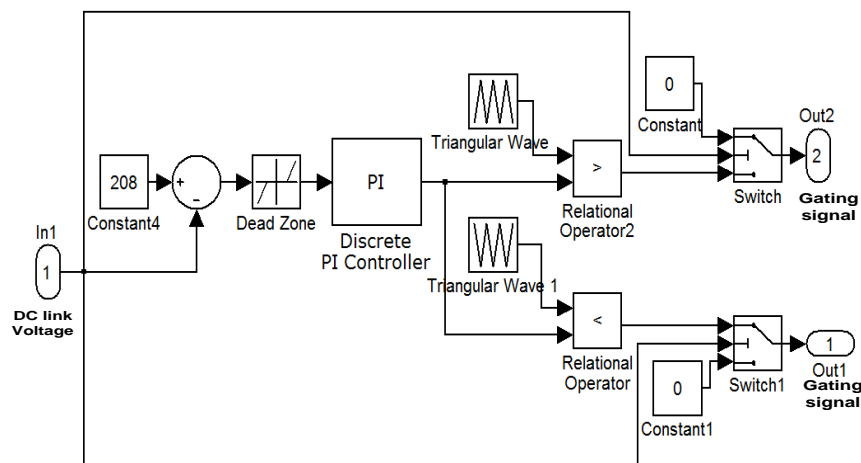


Figure 4.3. DC-DC Converter Controller

4.3 SIMULATION RESULTS

The simulation results of the bidirectional DC-DC converter when connected in the power conditioner circuit are presented. The voltage of the ultracapacitor and the DC link are shown in Figure 4.4. Note that the ultracapacitor does not discharge significantly over the 100 sec time interval. The DC-DC converter effectively maintains the voltage of the DC link relatively constant at a reference value.

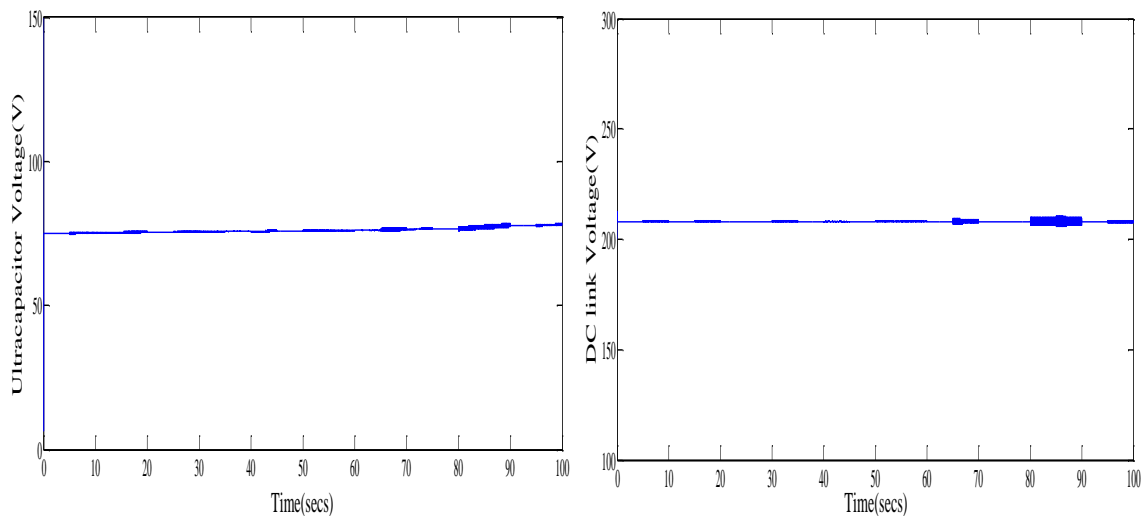


Figure 4.4. Voltage of the Ultracapacitor and the DC Link

4.4 CONSTRUCTION OF THE DC-DC CONVERTER

After the simulation results, the bidirectional DC-DC converter and the single phase VSI are constructed. These converters are integrated in the construction of the power quality conditioner. The main objective of the bidirectional DC-DC converter is to maintain the voltage of the DC link relatively constant at a fixed reference value. The bidirectional DC-DC converter acts a buck converter in one direction and as a boost converter in the other direction. Power MOSFETS, IXFK80N50P are used as the switching devices in the DC-DC converter circuit. The flowchart showing the construction of the DC-DC converter is shown in the Figure 4.5.

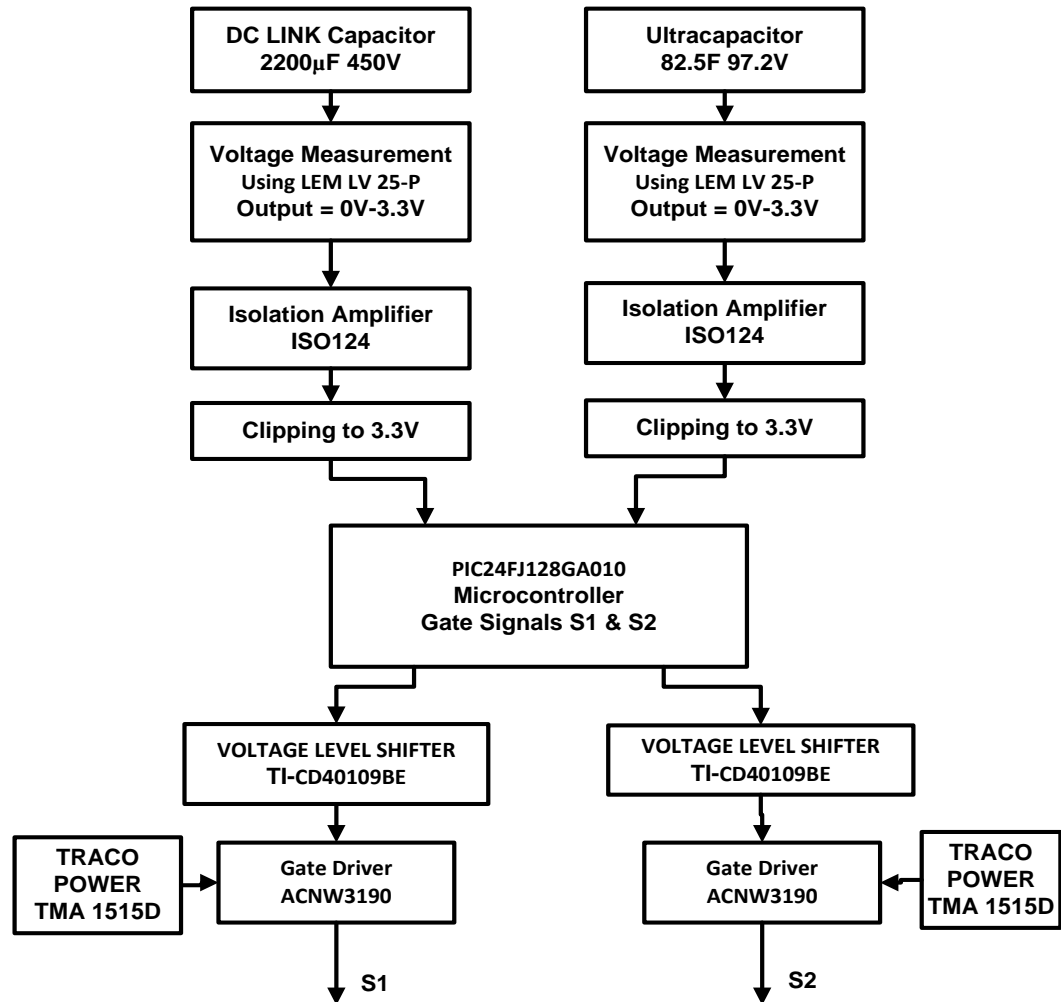


Figure 4.5. Flowchart Showing the Construction of the DC-DC Converter

The Microchip PIC24FJ128GA010 microcontroller along with the Explorer16 development board is used in implementing the control scheme and to obtain the gate signals for the MOSFETs in the bidirectional DC-DC converter. LEM LV 25-P voltage sensors are used for measuring the voltages of the DC link and the ultracapacitor. The ACNW3190 5.0 Amp High Output Current Gate Drive optocoupler is used to drive the MOSFETs. The high power MOSFETs are used as switching devices in the circuit and

are mounted on a heat sink. A TP-75C DC power supply is used to supply power to the LEM sensors and gate drivers. The voltage measurement circuits and the gate driver circuits are built on the vector board and are soldered permanently. The high current inductor used in the circuit is manufactured by West Coast Magnetics. Two Maxwell ultracapacitor modules of nominal capacitance 165F and rated voltage 48.6V are connected in series and they are connected to one side of the DC-DC converter.

4.4.1 PIC Microcontroller The Microchip microcontroller PIC24FJ128GA010 along with the Explorer16 development board is used to implement the control of the DC-DC converter and to obtain gate signals for the MOSFETs in the DC-DC converter. MPLAB ICD3 in-circuit debugger is used to program and verify the target device. The program for implementing the control logic is written in C language. The microcontroller operates and sends the gate signals to the MOSFET drivers depending on the control logic. The inbuilt potentiometer on the development board, which produces variable voltage from 0V to 3.3V, is used to test the microcontroller operation after programming the device. After testing, the microcontroller is connected in the circuit to obtain the closed loop control and the respective MOSFET gate signals. The PIC24FJ128GA010 microcontroller is a 16 bit flash general purpose microcontroller. It has a 10 bit 16 channel ADC module and five 16 bit PWM output compare modules. It has also many peripheral features such as UART and parallel master slave port etc., It is a 100 pin device with PIM structure, so it can easily fit into the Explorer 16 development board. The voltages of the DC link and ultracapacitor are measured using the LEM 25-P voltage sensors and the analog values are fed to the ADC module in the microcontroller through a isolation amplifier ISO124P. When the ADC module is enabled the conversion starts and the converted digital values are stored in a ADC Buffer. Thus obtained, digital values are used to perform the control logic. The reference value for the controller is set in the program. After calculating the error from the voltage of the DC link and the reference value, the error signal is passed through a PI control scheme. Depending on this error signal, the output compare modules in the microcontroller are enabled and they operate to give the desired gate signals. The operation of the microcontroller is presented in the flowchart as shown in the Figure 4.6.

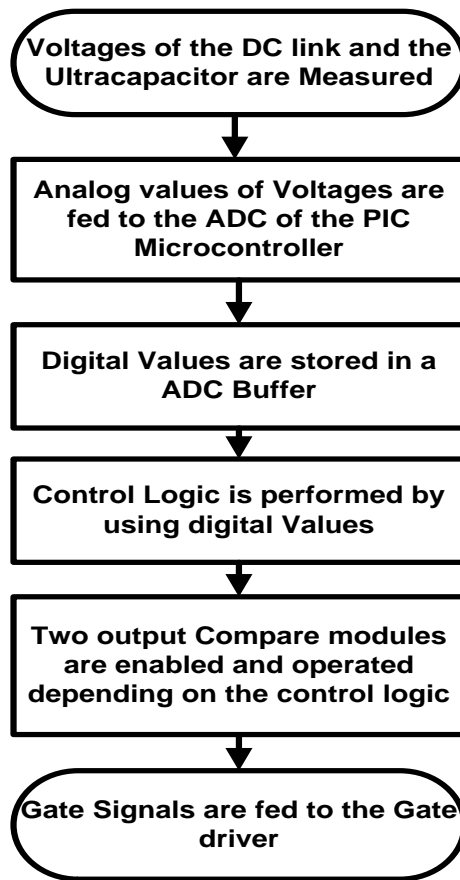


Figure 4.6. Flowchart Showing the Operation of the Microcontroller

The control logic of the DC-DC converter is described in section 4.2. The main objective of the DC-DC controller is to maintain the voltage of the DC link relatively constant at the reference value. The control strategy of the converter is shown in the Figure 4.2. Whenever the voltage of the DC link raises above the reference value, gating signal obtained from the output compare module 4 is given to the MOSFET Q1 and Q2 is turned off. In this case, the DC-DC converter acts in buck mode reducing the DC link voltage. Whenever, the DC link voltage falls below the reference value then, gating signal obtained from the output compare module 5 is given to MOSFET Q2 and Q1 is turned off. In this case, the DC-DC converter acts in boost mode, increasing the DC link voltage.

4.4.2 Voltage Measuring Circuit The voltages of the DC link and the ultracapacitor are measured using voltage sensors, LEM LV 25-P. The voltage measuring circuit is shown in Figure 4.7. For measuring DC link voltage, the measurement circuit is designed such that it measures the voltage in the range of 0V-400V and produces the measured output voltage in the range of 0V-3.3V. In this case R1 is chosen as 40k Ω and R2 is chosen as 132 Ω . Similary, the ultracapacitor voltage measurement circuit is designed such that it measures the voltage in the range of 0V-120V and produces the measured voltage in the range of 0V-3.3V. In this case R1 is chosen as 12k Ω and R2 is chosen as 132 Ω . These measured analog values are fed to the ADC module of the microcontroller through the isolation amplifier. The power to the LEM voltage sensors are supplied from a TP-75C DC power supply. The voltage measurement circuits are soldered on the vector board. The resistors selection calculation is shown below.

Primary nominal RMS current=10mA

Secondary nominal RMS current=25mA

Ultracapacitor Voltage measurement resistors selection is shown below

Output Range = 0V-3.3V

$R2 = 3.3V/25mA = 132\Omega$

Input Range = 0V-120V

$R1 = 120/10mA = 12k\Omega$

DC link Voltage measurement resistors selection is shown below

Output Range = 0V-3.3V

$R2 = 3.3V/25mA = 132\Omega$

Input Range = 0V-400V

$R1 = 400/10mA = 40k\Omega$

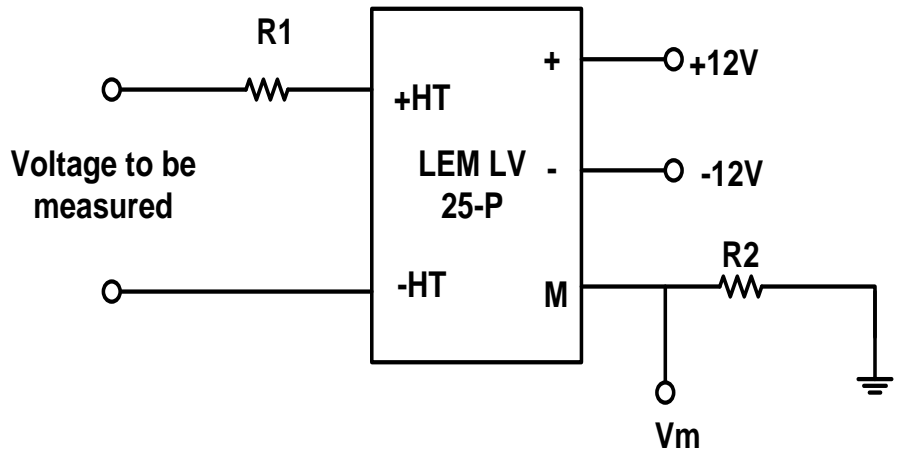


Figure 4.7. Voltage Measuring Circuit

The measured signal from the voltage sensor is passed through an isolation amplifier ISO124P in order to provide isolation. Table 4.1 presents the test results of the ultracapacitor voltage measuring circuit. Table 4.2 presents the test results of the DC link voltage measuring circuit.

Table 4.1. Ultracapacitor Voltage Measurements

Ultracapacitor Voltage	LEM Voltage Sensor o/p	Voltage after Isolation Amplifier
110V	3.02V	3.015V
30V	0.835V	0.833V

Table 4.2. DC Link Voltage Measurements

DC link Voltage	LEM Voltage Sensor o/p	Voltage after Isolation Amplifier
390V	3.223V	3.221V
30V	0.247V	0.245V

4.4.3 Gate Driver Circuit The gate driver circuit is built using Avago technologies, ACNW3190 5.0 Amp High Output Current Gate Drive optocoupler is shown in the Figure 4.8. The 15V isolated voltage is required for the driver as supply voltage, which is supplied by a TRACO power DC-DC converter IC, TMA 1515D. The input to the driver should be 5V signal, so a buffer is used to amplify the gate signals obtained from the microcontroller from 3.3V to 5V. The gate driver has a 5A maximum peak output current. Two gate drivers are used for driving the two MOSFETS. The gate driver circuits are soldered on the vector board.

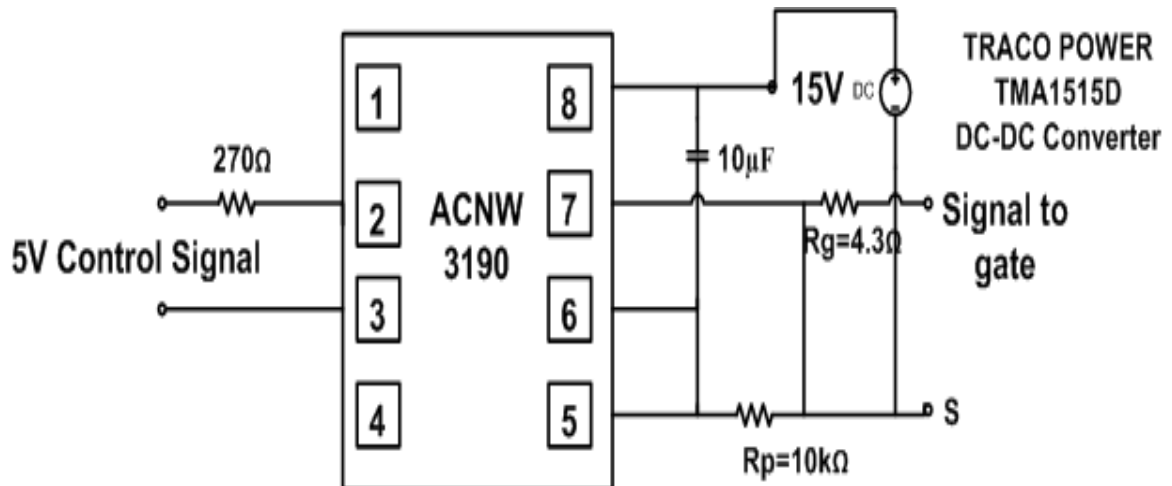


Figure 4.8. Gate Driver Circuit

4.5 HARDWARE RESULTS

The experimental setup of the bidirectional DC-DC converter and the different components used in the construction of the DC-DC converter are shown in Figure 4.9.

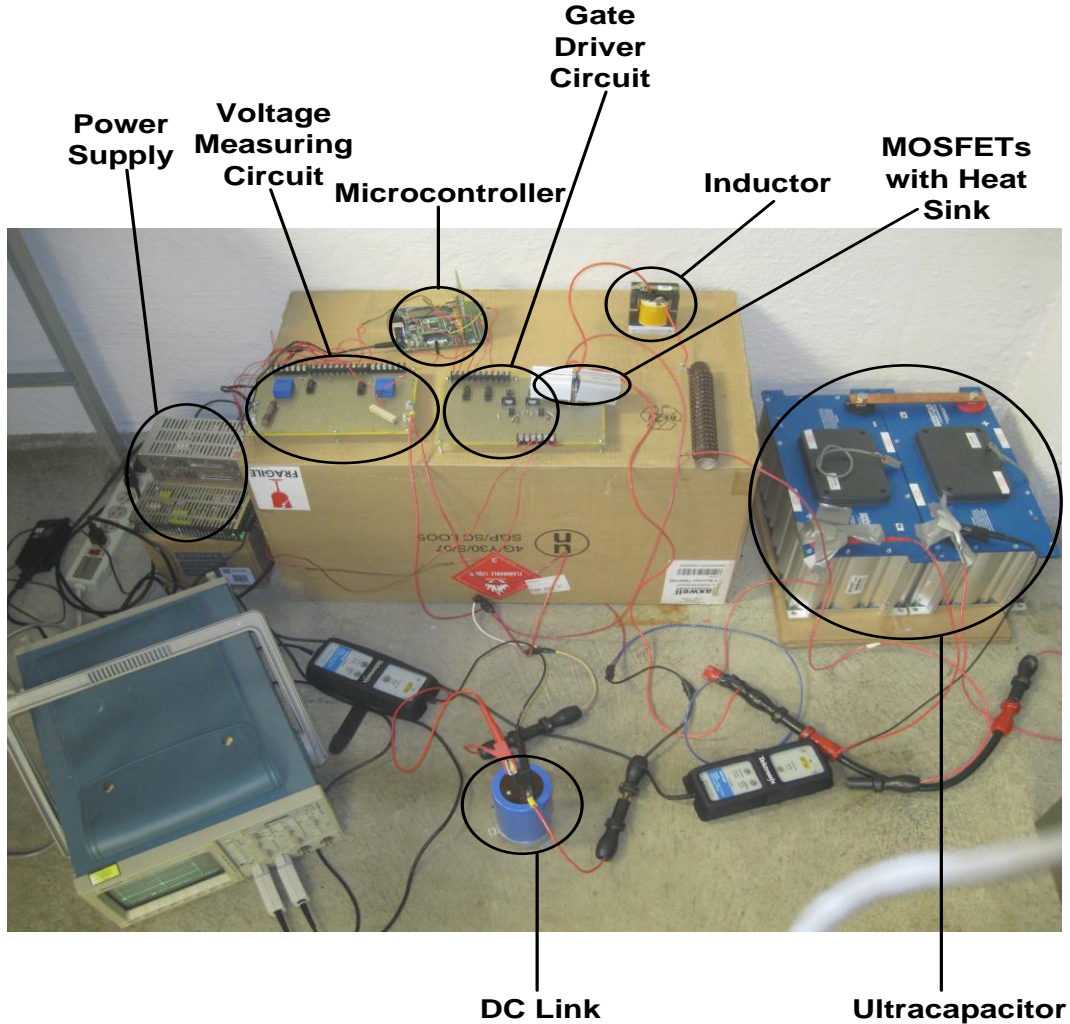


Figure 4.9. Experimental Setup of the Bidirectional DC-DC Converter

The gate signals that are obtained from the microcontroller in buck and boost modes are shown in the Figure 4.10. In buck mode, the MOSFET Q1 operates with the obtained gate signals from output compare module 4 and Q2 does not operate. In boost mode, the MOSFET Q2 operates with the obtained gate signals from output compare module 5 and Q1 does not operate. These gate signals are passed through the gate driver circuits in order to drive the MOSFETs. The signals from the gate drivers in buck and boost modes are shown in the Figure 4.11.

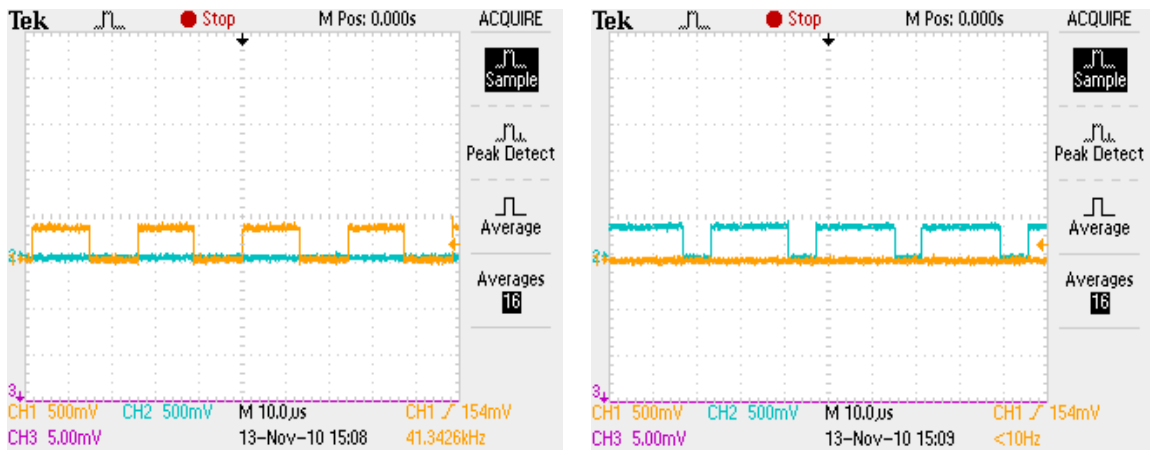


Figure 4.10. Gate Signals in Buck Mode and Boost Mode

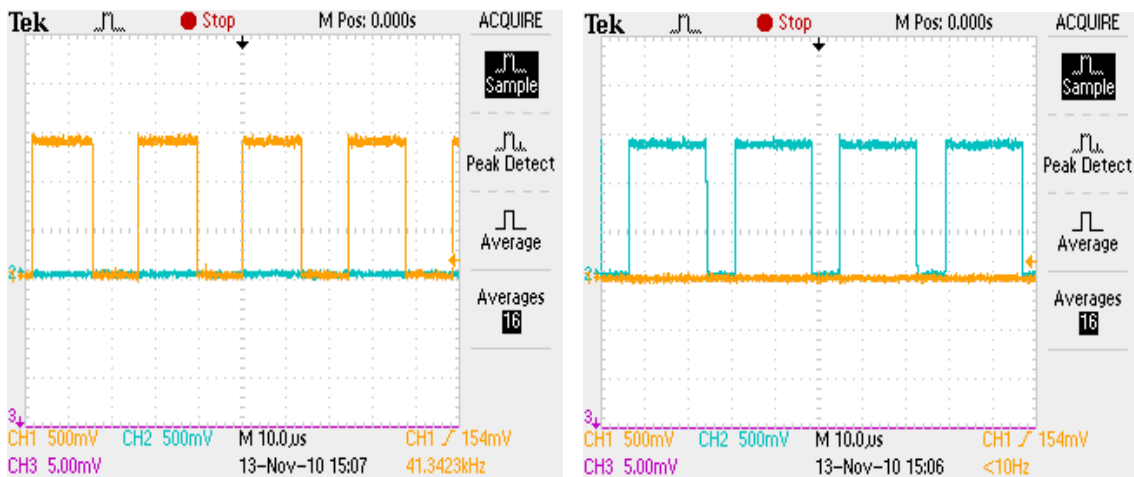


Figure 4.11. Gate Signals from Driver in Buck Mode and in Boost Mode

The results of the bidirectional DC-DC converter are presented in Figure 4.12 and Figure 4.13. The voltage of the DC is maintained at 120V as shown in Figure 4.12. The voltage of the ultracapacitor is shown in the Figure 4.13. These results show that DC-DC converter is good at maintaining the voltage of the DC link at a constant reference value. The conditioner is initially tested by connecting it between the output line and the neutral of the wind turbine. In this case, the voltage of the DC link is maintained at 120V and the results are shown for this case. When, the conditioner is tested by connecting between the two output lines of the wind turbine, the DC link voltage is maintained at 208V

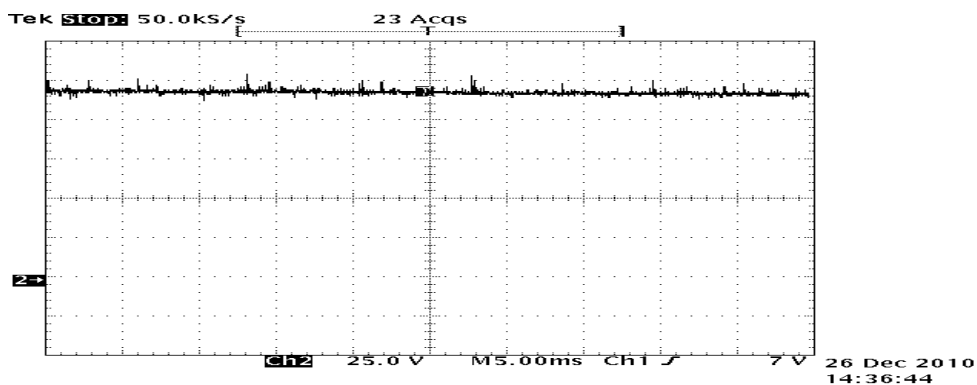


Figure 4.12. Voltage of the DC Link

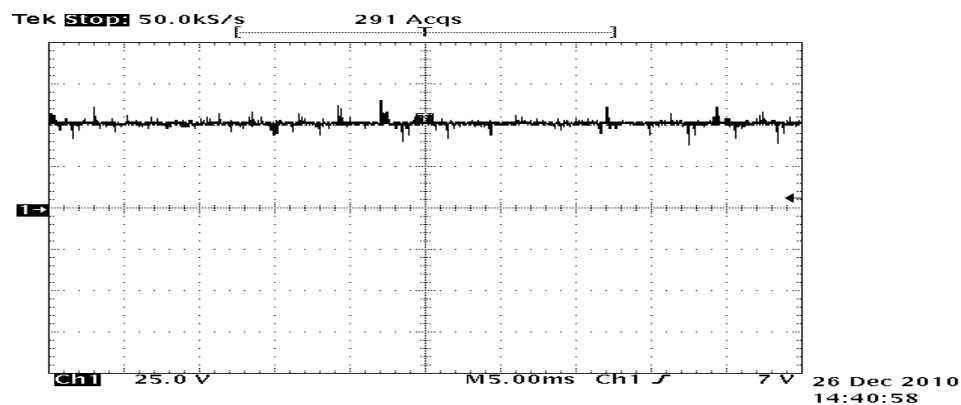


Figure 4.13. Voltage of the Ultracapacitor

5. SHUNT INVERTER

5.1 TOPOLOGY OF THE VSI

A full-bridge IGBT based inverter topology is used in this application. The full-bridge inverter consists of four switching devices, which are connected to form the full-bridge inverter circuit shown in Figure 5.1. The gating signals for the IGBTs are obtained by the pulse width modulation controller. Anti-parallel diodes are connected across the power IGBTs to protect the devices and to provide the power flow in the reverse direction [12], [13]. The voltage source inverter is connected in shunt to the line acts as a current source, injecting or drawing the compensating current from the line [14]. The shunt inverter is connected to the line through a series interference RL filter, which reduces the unwanted harmonics. The filter provides smoothing and isolation from high frequency components. On the other side, the simple full-bridge line connected inverter is connected to the DC link. The injecting current is in phase with the line voltage to have a unity power factor.

The VSI operates in the following two modes:

- Mode 1: When the wind power is greater than the desired value, the converter acts like a rectifier drawing the power from the line and charging the DC link capacitor.
- Mode 2: When the wind power is less than the desired value, then the converter acts like the VSI injecting power into the line by discharging the DC link capacitor.

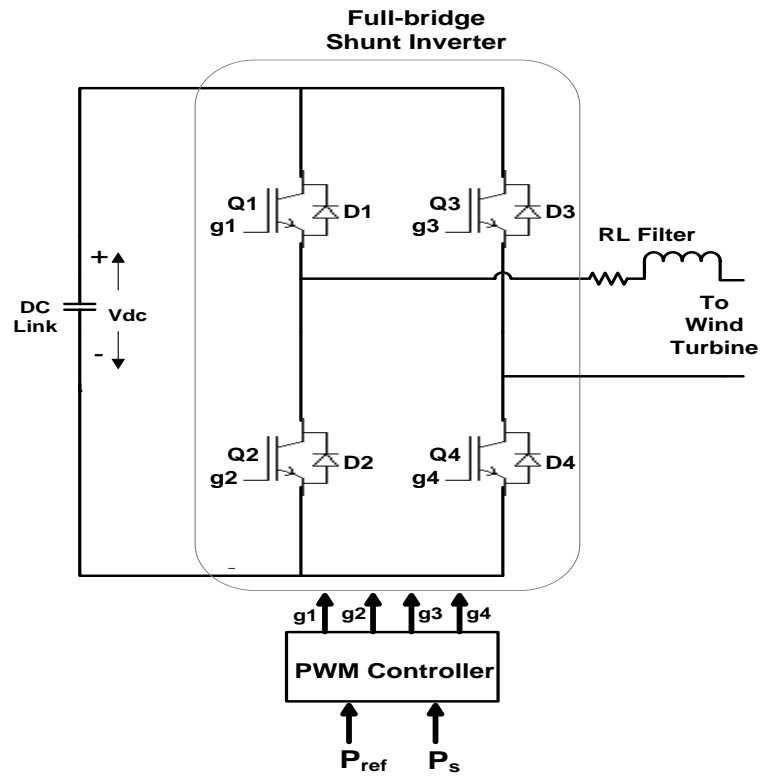


Figure 5.1. Circuit Diagram of the Shunt Inverter

5.2 CONTROL OF THE SHUNT INVERTER

The variable wind power is passed through a low pass filter to get a smoothing reference signal for the inverter controller. The output of the low pass filter is given to the shunt inverter controller as the reference value [15]. The reference signal P_{ref} is obtained as below

$$P_{ref} = \frac{1}{1+ST} * P_{wind} \quad (6)$$

where T is the time constant of the filter. The smoothing performance of the wind turbine output power depends on the time constant of a low pass filter. The time constant of the low pass filter is in the range of several seconds and is tuned to provide the desired smoothing. The power fluctuation is smoothed by drawing or injecting the difference of the reference power and the variable wind power.

A pulse width modulation (PWM) controller is used to control the switching of the power devices in the full-bridge shunt inverter. The inverter control strategy is shown in the Figure 5.2. PWM controller controls the magnitude and phase of the output of the inverter. The advantage of the PWM is both the magnitude and phase of the output can be controlled. Modulation is achieved by comparing the sinusoidal waveform of certain frequency and amplitude to a high frequency triangular carrier waveform. The output frequency of the shunt inverter depends on the frequency of the sinusoidal waveform. The output current waveform shape of the inverter depends on the switching frequency and the filter inductor. The damping in the circuit depends on the filter connected to the inverter output. A bipolar PWM technique is used in this work to control the switching of the inverter. The bipolar switching sequence used is:

- If $V_{\text{cont}} > V_{\text{tri}}$, then Q1 is on
- If $V_{\text{cont}} < V_{\text{tri}}$, then Q2 is on
- If $-V_{\text{cont}} > V_{\text{tri}}$, then Q3 is on
- If $-V_{\text{cont}} < V_{\text{tri}}$, then Q4 is on

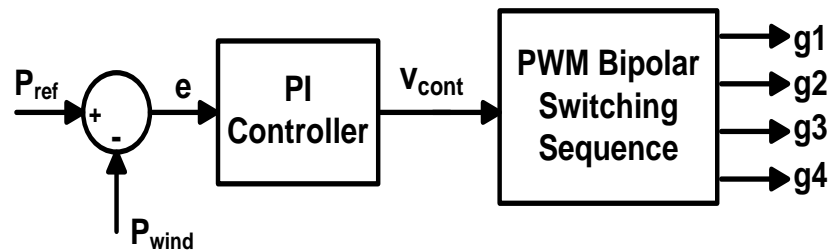


Figure 5.2. Shunt Inverter Control Scheme

5.3 CONSTRUCTION OF THE SINGLE PHASE VSI

5.3.1 Measurement Circuit The line voltage and line current are measured using the LEM 20P voltage sensor and bell CLN 50 current sensor. The voltage measurement circuit is described in section 4.4.2. The voltage and current sensors are mounted before and after the conditioner connection to assess the performance of the conditioner.

5.3.2 Signal Shaping Circuit The sensor signals are sent to the DSP A/D converter ports through a shaping circuit as shown in Figure 5.3. The shaping circuit has to translate the scaled signal from -6 to 6 volts to 0 to 3 volts because the DSP is CMOS-based and only accepts 0-3 volts. The shaping circuit is built with LF 347 operational amplifier. The 1.5V is supplied from the LM317 adjustable regulator as shown in the Figure 5.4. 5V is given as supply to the LM317. By choosing the appropriate resistors, the 1.5V signal is obtained at the output. In the signal shaping circuit, the resistors are adjusted such that the output signal always lies between 0V-3V for -6V to 6V input. The signal shaping circuit is tested by giving a sinusoidal signal of frequency 60Hz and amplitude 5V. The result is shown in Figure 5.5

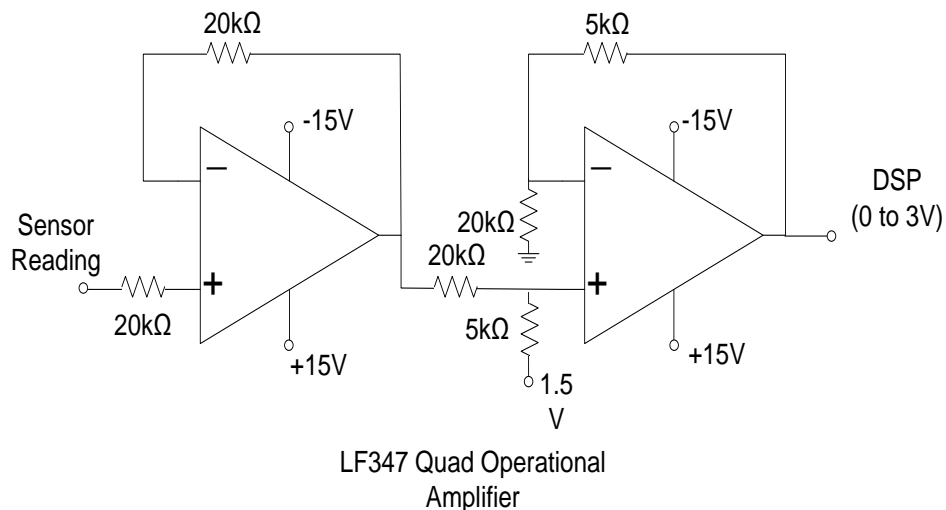


Figure 5.3. Signal Shaping Circuit using Operational Amplifier

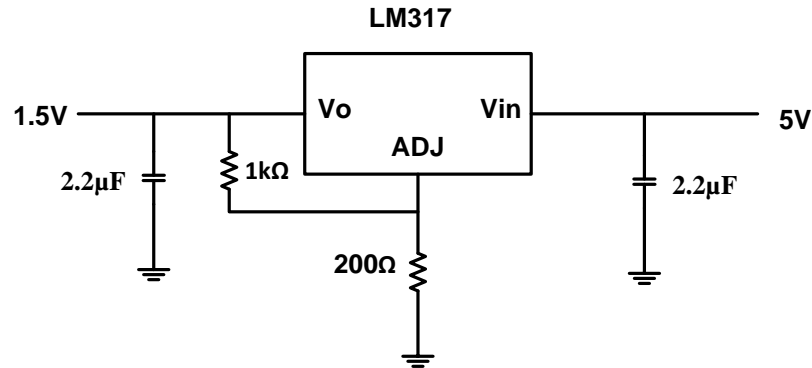


Figure 5.4. Voltage Regulation Circuit using LM317

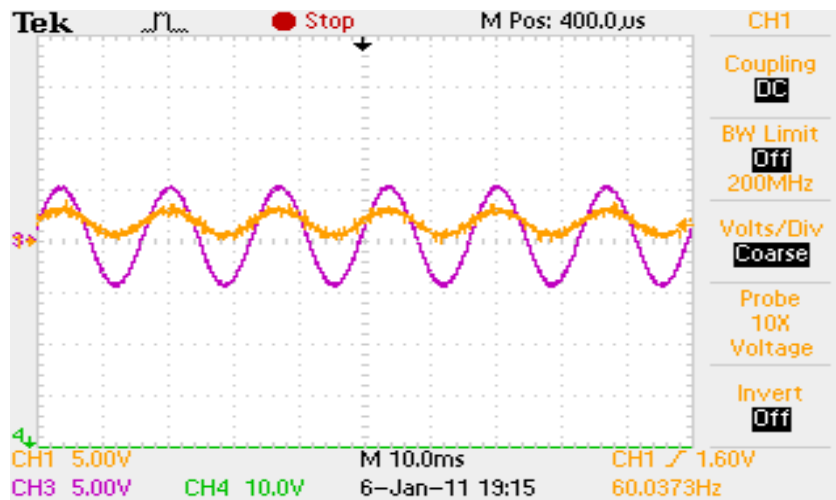


Figure 5.5. Signal Shaping Circuit Input and Output

5.3.3 Digital Signal Controller A TI TMDSDOCK28335 DSP is used to obtain the gate signals for the IGBTs in the shunt inverter circuit. The DSP is programmed using the code composer studio. The main loop program structure is as shown in the Figure 5.6. Initially the system initialization such as system clock and GPIO pin assignment is done. Then ADC and PWM modules are initialized and timers are enabled to start A/D converter and to start PWM generation. The main loop works until the program is halted.

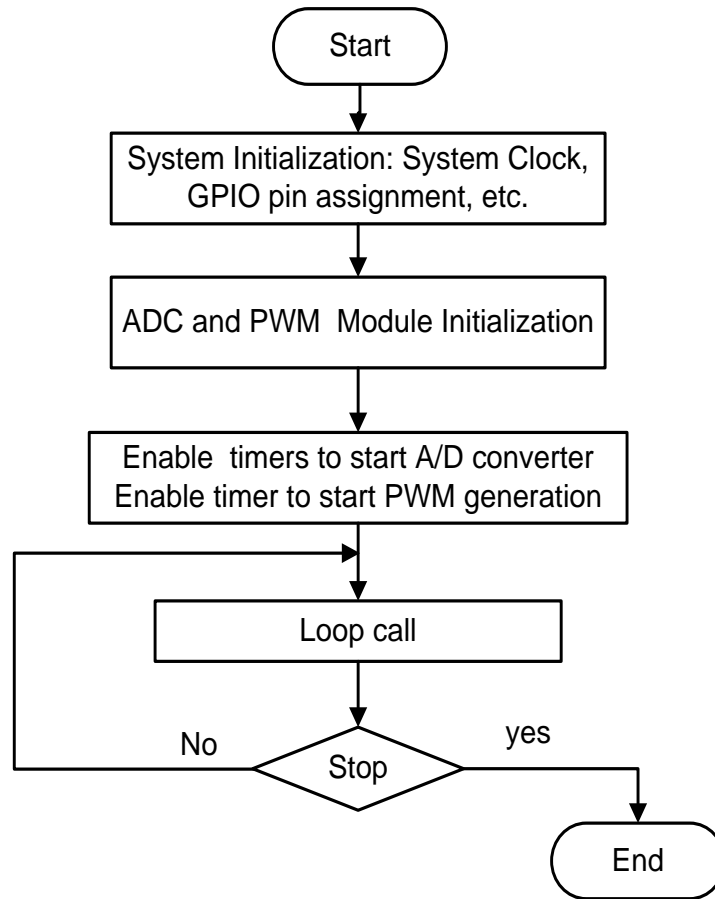


Figure 5.6. DSP Main Loop Program Structure

The voltage and current sensor signals from the signal conditioning board are given to the ADC ports in the DSP. Before implementing the program in the physical setup, the ADC module is tested. Figure 5.7 presents the test results of the ADC converters 1 and 2 in the module. For testing, the PWM signals are passed through the ADC converters. The converted digital values are seen in the watch window. The ADC module converts these analog values to digital values. The control logic is performed using these digital values and finally it is used in the PWM generation.

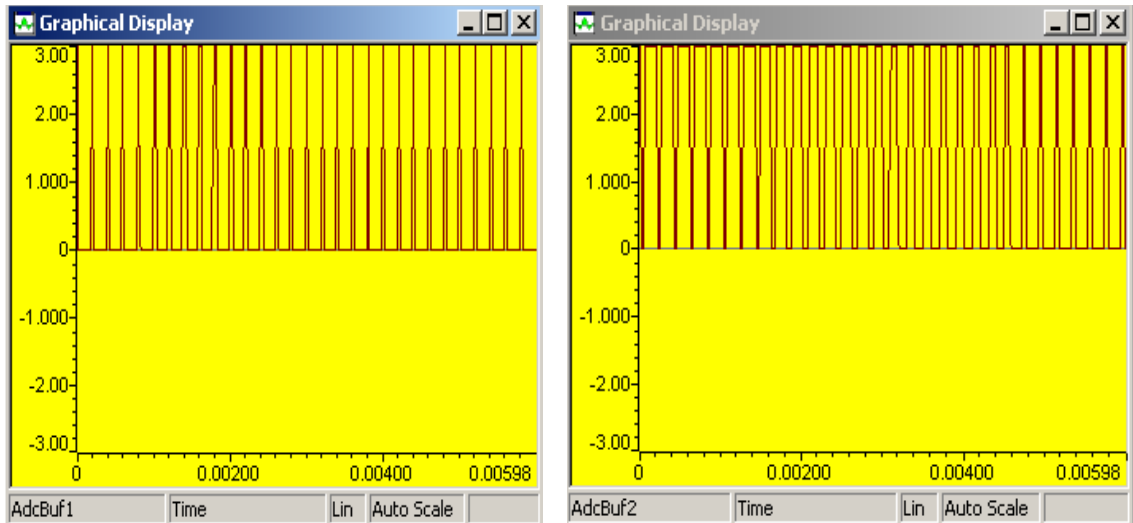


Figure 5.7. Test Results of the ADC Converter 1 and 2 in the Module

The variable sensor signals are passed through a low pass filter to get a smoothing reference signal for the inverter controller. The output of the low pass filter is given to the shunt inverter controller as the reference value [15]. The smoothing performance of the wind turbine output power depends on the time constant of a low pass filter. The time constant of the low pass filter is in the range of several seconds and is tuned to provide the desired smoothing. The low pass filter is implemented in the DSP using the programming. For testing, the time constant of the filter is set at 0.5 sec and the PWM signal is given as an input which varies between 0V and 3 V. The low pass filter result is shown in the Figure 5.8.

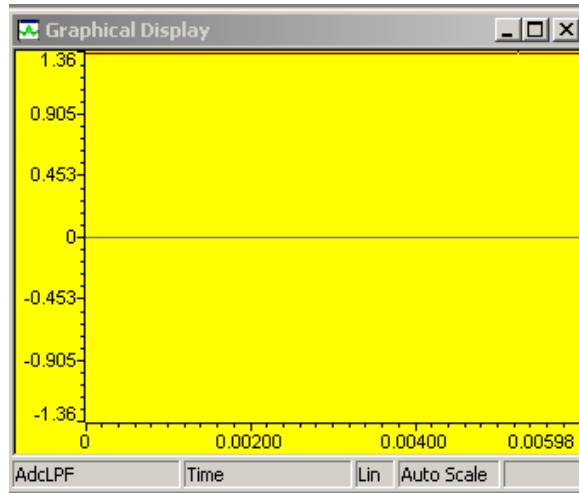


Figure 5.8. Test Result of the Low Pass Filter

5.3.4 PWM Signal Generation Sinusoidal pulse width modulation (PWM) is used to generate the IGBT switching signals. In sinusoidal PWM, a high frequency triangle carrier waveform is compared against a reference sinusoidal waveform with desired magnitude and frequency. Respective switching signal is sent to the IGBT. The DSP-based PWM control signal generation is capable of providing 4 switching signals to the converters with adjustable dead time. Dead time is the time after each event during which the system is not able to record another event if it happens.

5.4 HARDWARE RESULTS

The gate signals obtained from the DSP is shown in the Figure 5.9. A dead time is also introduced in order to avoid possible short circuits. The dead time can be clearly seen in Figure 5.9.(b); these gate signals are passed through gate drivers before being given to IGBTs. The gate signals from the gate drivers with dead time are shown in the Figure 5.10.

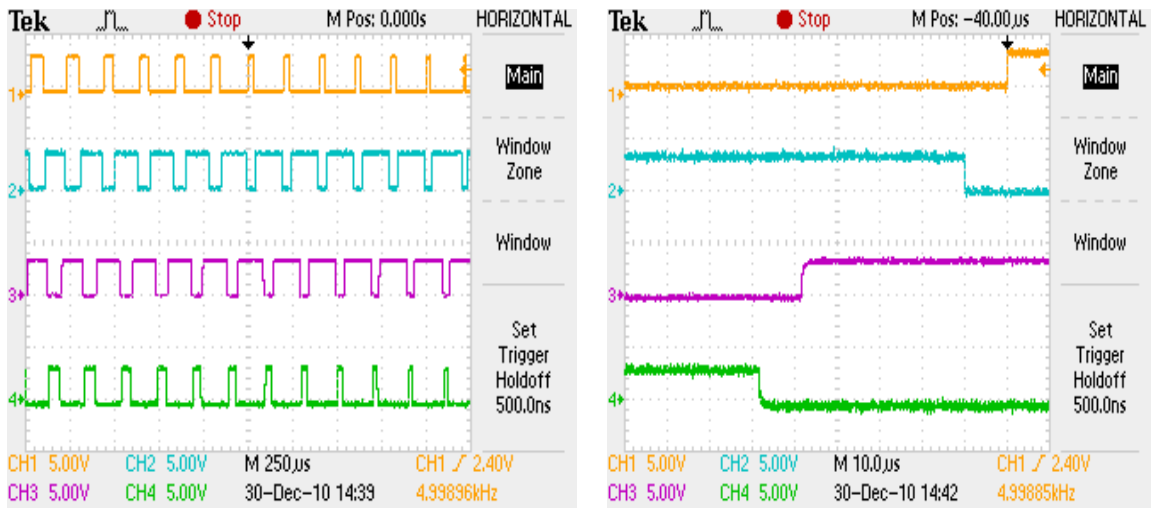


Figure 5.9. Gate Signals from the DSP and Dead Time Implemented

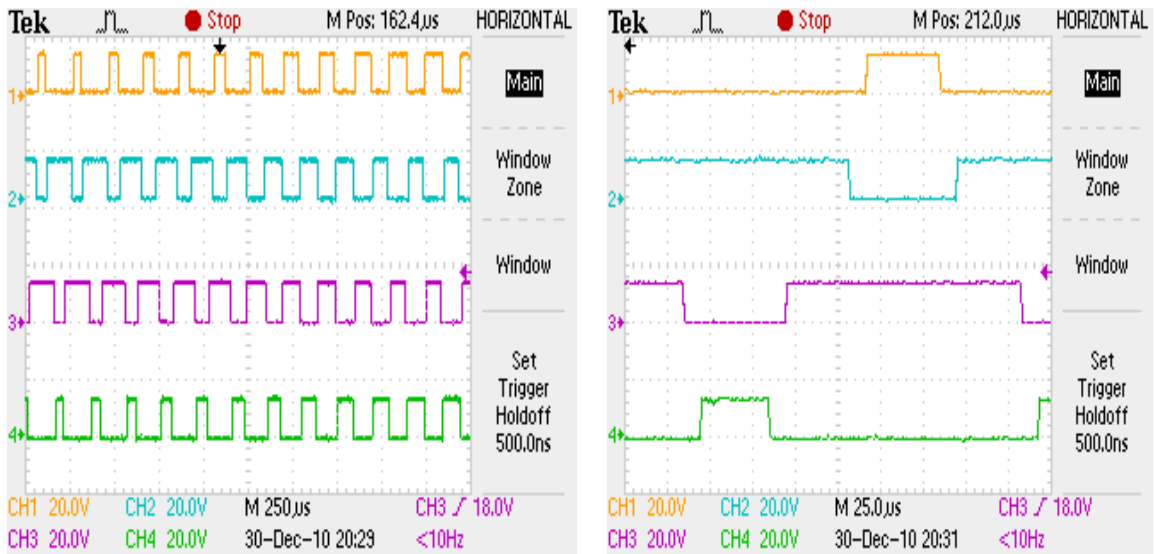


Figure 5.10. Gate Signals from the Driver and Dead Time Implemented

The experimental setup and different components in the construction of the single phase shunt inverter are shown in the Figure 5.11. A SEMIKRON SK 30 GBB 066 T IGBT module is used as the switching devices for the circuit. A 2.5mH inductor is used as the output filter of the shunt inverter. A TI TMDSDOCK28335 DSP is used in the closed loop control of the shunt inverter. The current and voltage sensors measures and sends signals to the DSP through the signal shaping circuit. DSP drives the IGBTs with the ACNW3190 drivers as described in section 4.4.3.

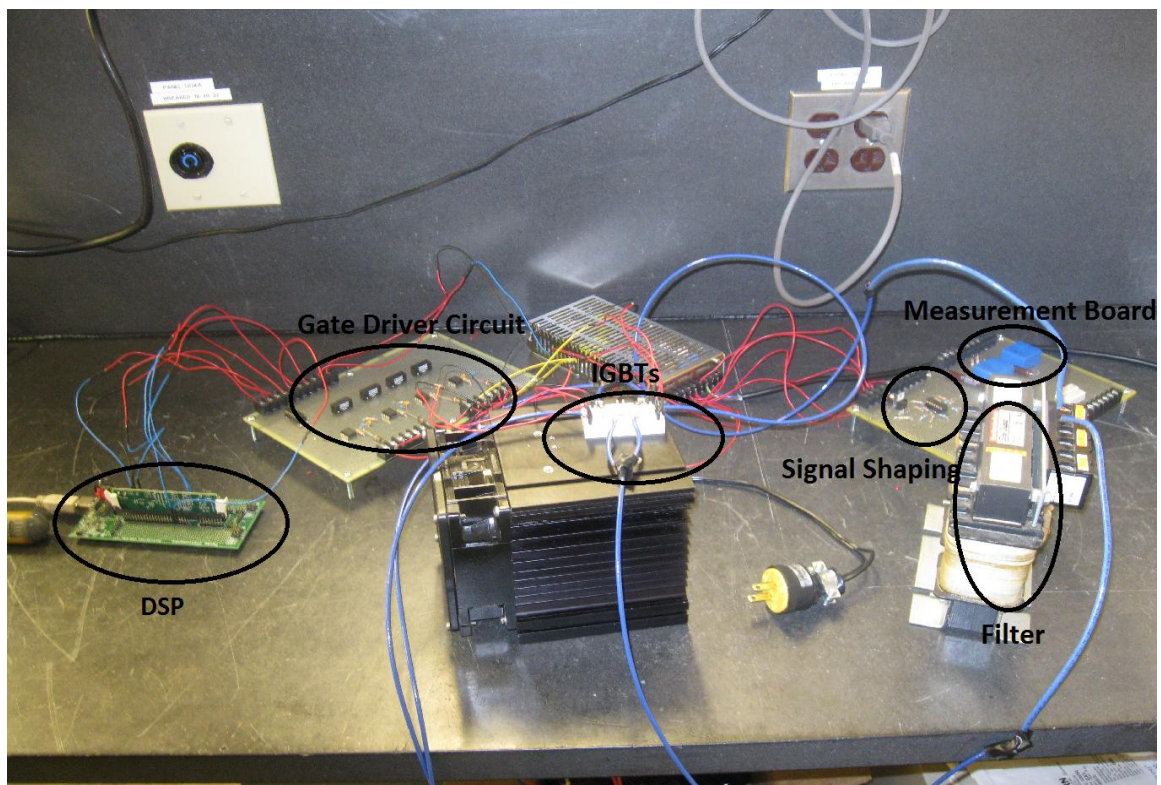


Figure 5.11. Experimental Setup of the Single Phase VSI

The constructed single phase inverter is tested in the laboratory with a small load. A 15V DC supply is given as input to the inverter for testing. A resistive load with the inductive filter is connected to the output of the inverter. The output voltage of the inverter without a filter is shown in Figure 5.12. The output voltage of the inverter with a RL filter is shown in Figure 5.13. The output current of the inverter with a RL filter is shown in Figure 5.14. The output voltage of the inverter with a LC filter is shown in Figure 5.15. The film capacitor of 500 μ F along with inductor is connected across the output of the inverter to get the good performance compared to the RL filter. The inverter is also tested when the DC link is given as the input. The DC-DC converter maintained the voltage of the DC link at 120V, it is given as the input to the inverter and the output of the inverter is given to the load through the filter.

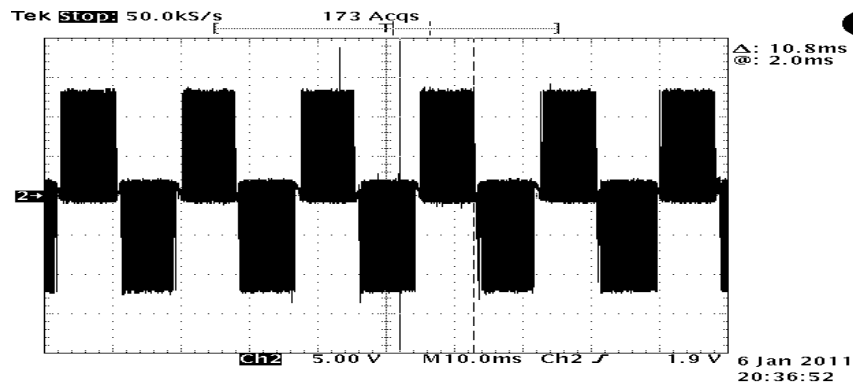


Figure 5.12. Output Voltage of the Inverter without Filter

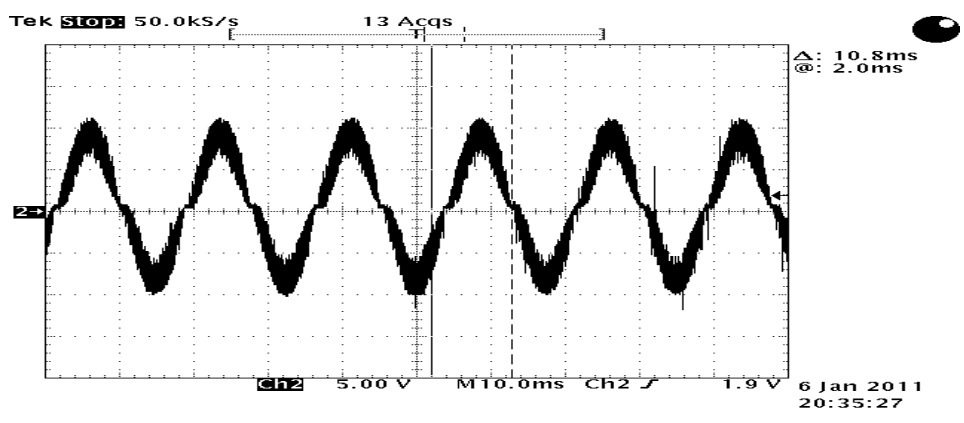


Figure 5.13. Output Voltage of the Inverter with RL Filter

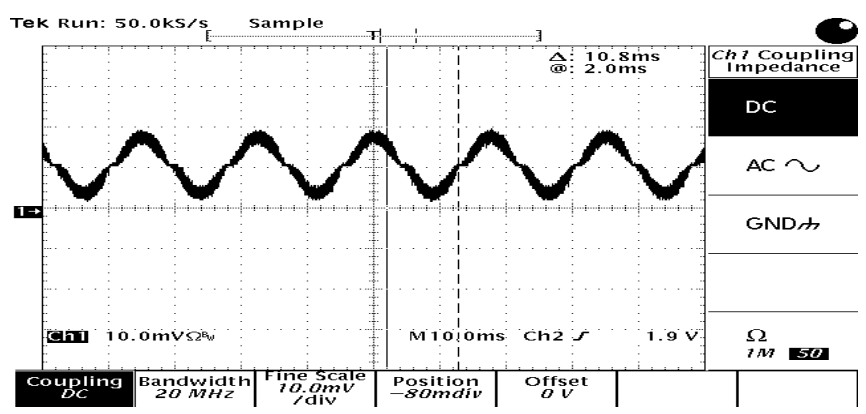


Figure 5.14. Output Current of the Inverter with RL Filter

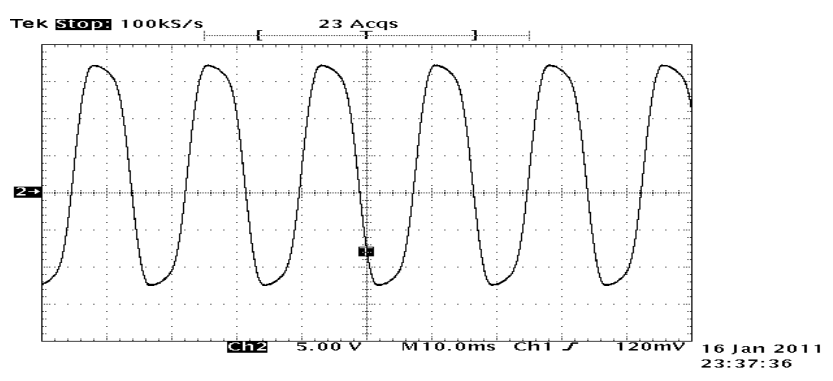


Figure 5.15. Output Voltage of the Inverter with LC filter

6. SYSTEM VALIDATION

6.1 SIMULATION RESULTS

The model of the proposed conditioner and its control has been developed using the SIMULINK software in MATLAB. Simulations are performed to investigate the performance of the power quality conditioner and its control. The important parameters used in the simulation are shown in Table 6.1.

Table 6.1. Simulation Parameters

Ultracapacitor	Nominal capacitance = 94F Initial voltage = 75V ESR = 12.5m Ω
DC-DC Converter	C1 = 9 μ F L1 = 26 μ H
DC Link	C = 2200 μ F Reference Value = 208V
DC-DC Converter Controller	K _p =.00167 K _i =10
Shunt Inverter Filter	R _{sh} =0.1 Ω L _{sh} =2mH

The variable output power of the wind turbine model developed in SIMULINK is shown in Figure 6.1. This model was developed to mimic the actual wind turbine active power output shown in Figure 2.2. The smoothed reference signal to the inverter controller is shown in Figure 6.2. The reference signal is obtained when the variable wind power is passed through a low pass filter with a large time constant. The simulation interval is 1500 sec in both cases.

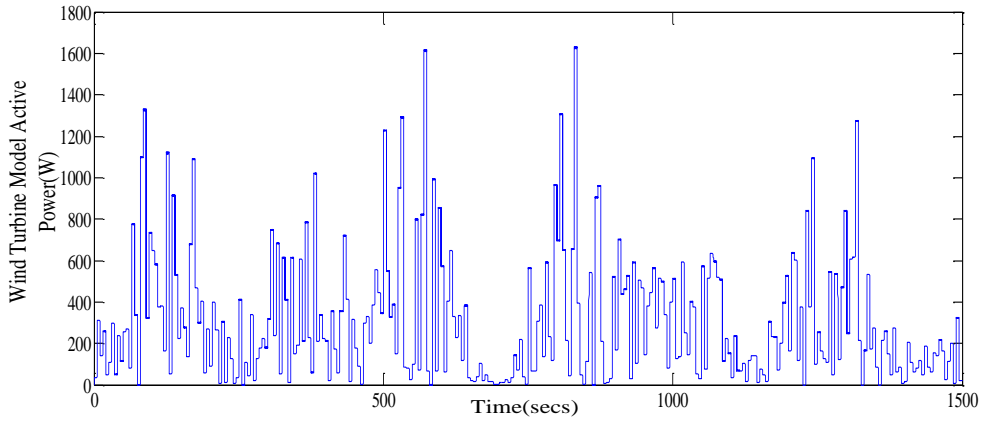


Figure 6.1. Modeled Active Power Output of the Wind Turbine

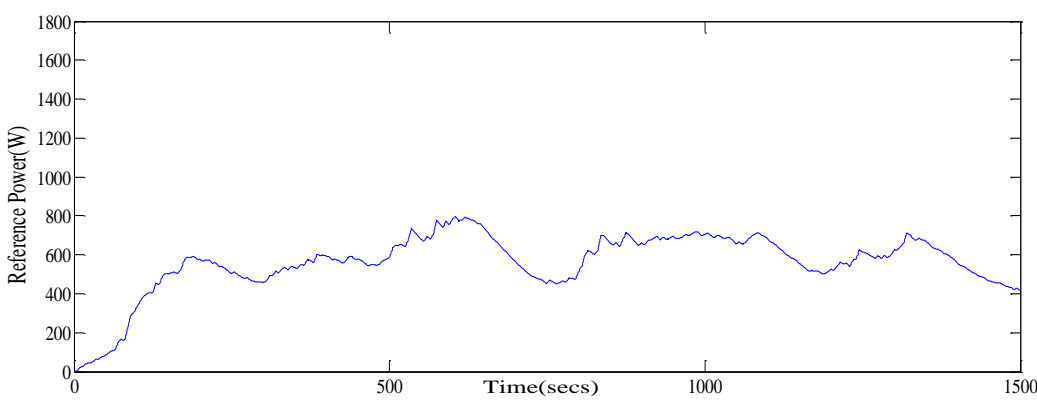


Figure 6.2. Reference Power Obtained from the Low Pass Filter

Figure 6.3 shows an expanded timescale of wind turbine output power for a 100 sec time interval. The expanded conditioner output is shown in Figure 6.4. When the active wind power is less than the reference value, the conditioner injects active power into the line. When the active wind power is greater than the reference value, the conditioner draws power from the line. The resulting smoothed power is shown in Figure 6.5. The smoothed power of the wind turbine is clearly following the reference signal.

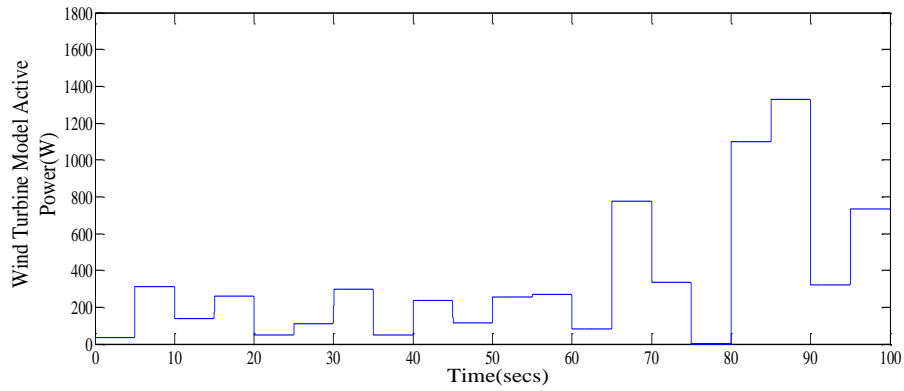


Figure 6.3. Active Power Output of the Wind Turbine Model

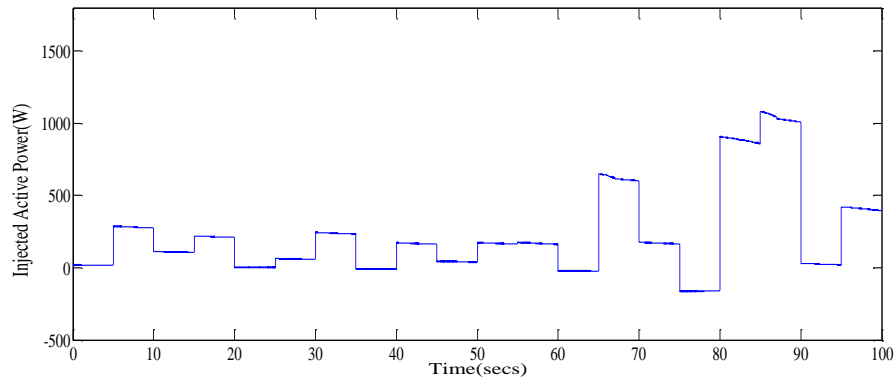


Figure 6.4. Conditioner Active Power

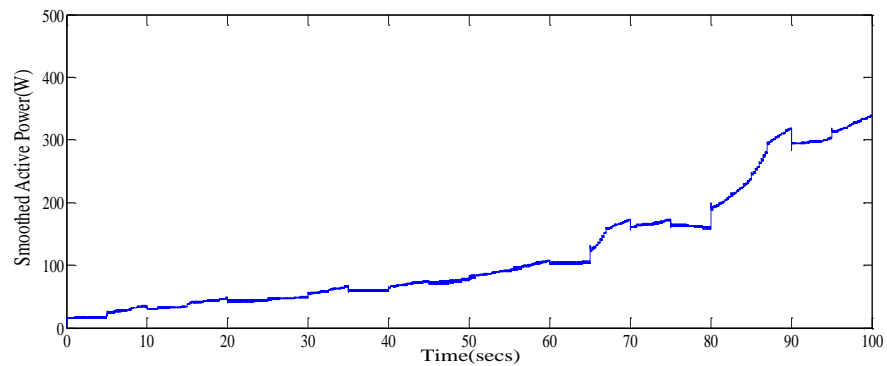


Figure 6.5. Smoothed Power at the Grid Interconnection Point

6.2 HARDWARE RESULTS

The experimental setup of the power quality conditioner is shown in Figure 6.6. It is tested in the laboratory with a load and then it is tested on the Skystream3.7 wind turbine installed in the campus.

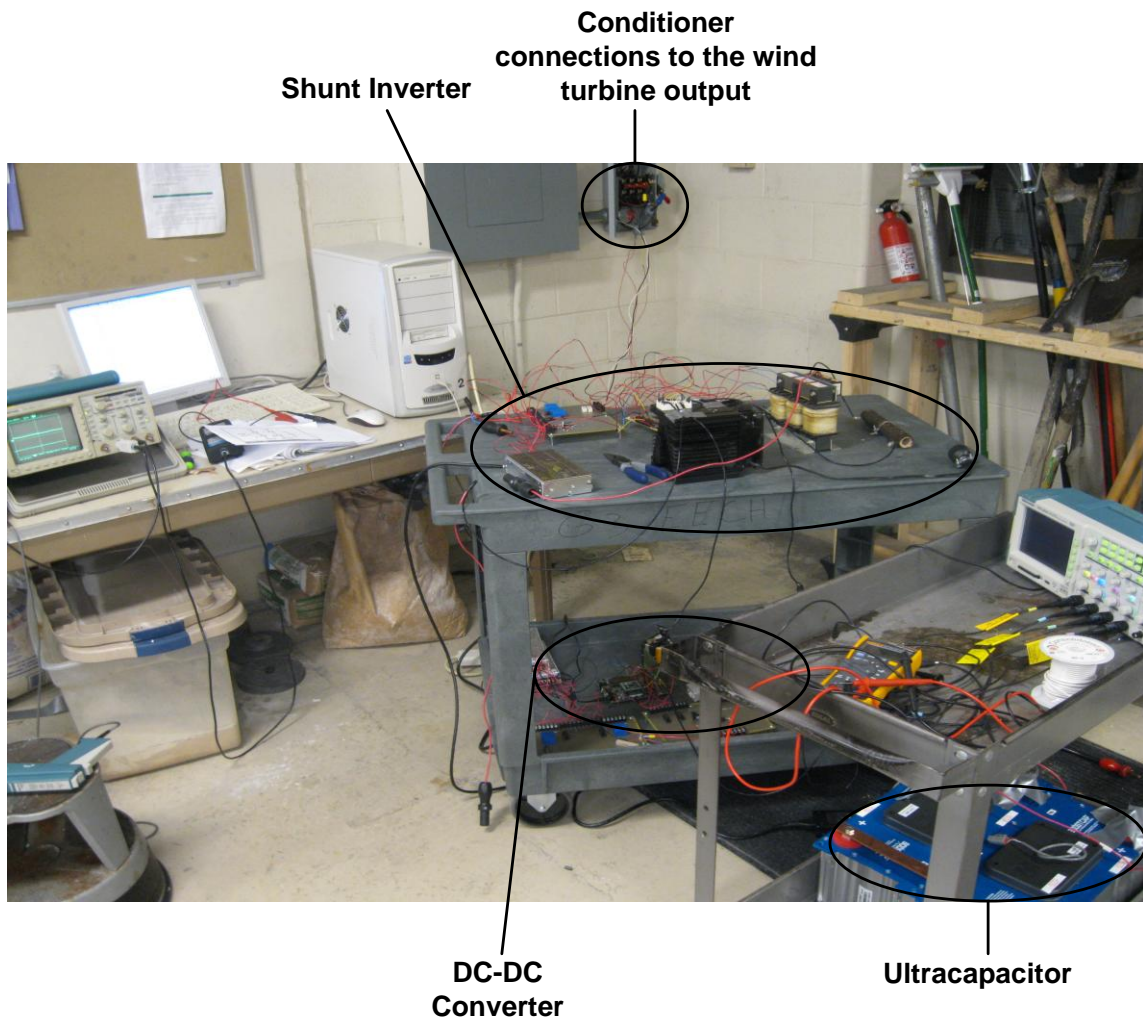


Figure 6.6. Experimental Setup of the Power Quality Conditioner

The power quality conditioner is connected in shunt between the output of the wind turbine and the grid interconnection point. The connections are shown in the Figure 6.7. The current sensors are installed before and after the connection of the conditioner to assess the performance of the conditioner as shown in the Figure 6.7. The RMS value of the voltage at the output of the wind turbine is shown in the Figure 6.8.

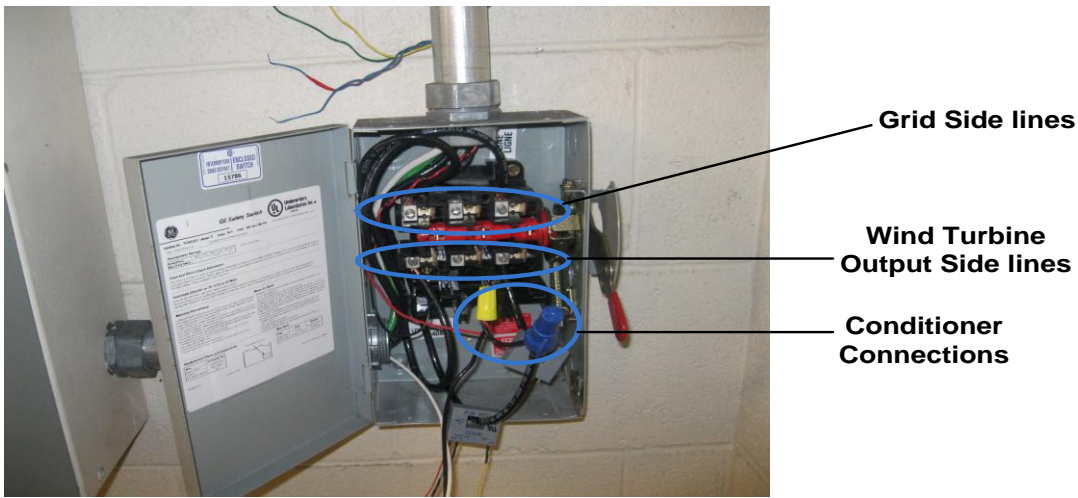


Figure 6.7. Power Quality Conditioner Connections to the Wind Turbine Output

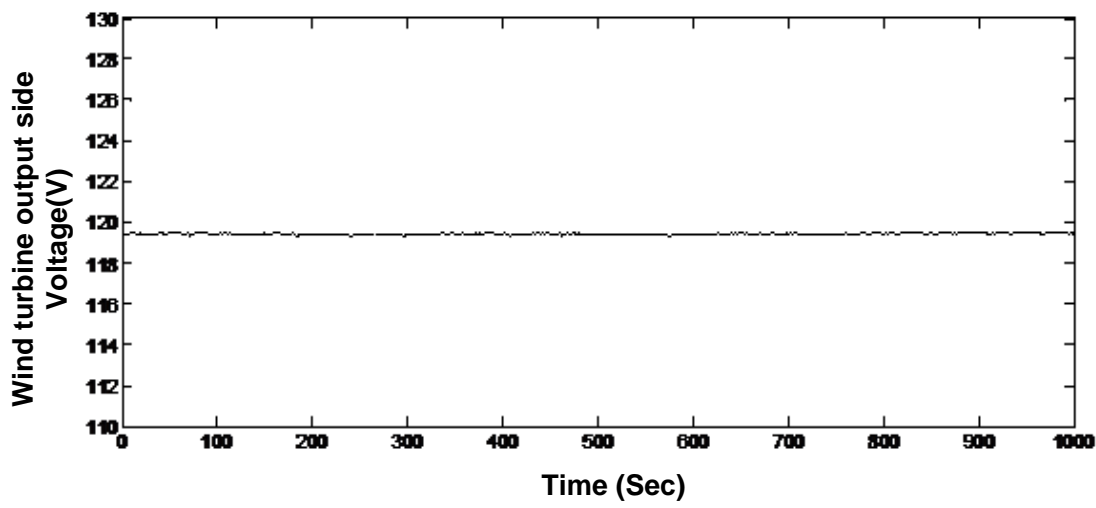


Figure 6.8. Measured RMS Voltage at the Output of the Wind Turbine

The RMS value of the current from the wind turbine is recorded for 1000 seconds is shown in the Figure 6.9. The RMS value of the current after connecting the conditioner is shown in the Figure 6.10. The RMS value of the Ultracapacitor voltage is shown in the Figure 6.11. The current after the conditioner connection is smooth compared to the wind turbine. The time constant we chose in the shunt inverter control is good in smoothing the power. From the figure 6.11, ultracapacitor is charging, when the conditioner is drawing the power and it is discharging, when the conditioner injects power into the line. The measured signals from the voltage and current sensors are connected to the National Instruments data acquisition module, NI USB-6009, which sends the data to a computer through a USB port. The data is recorded using the signal express software. It stores the data in the excel sheet and then it is plotted.

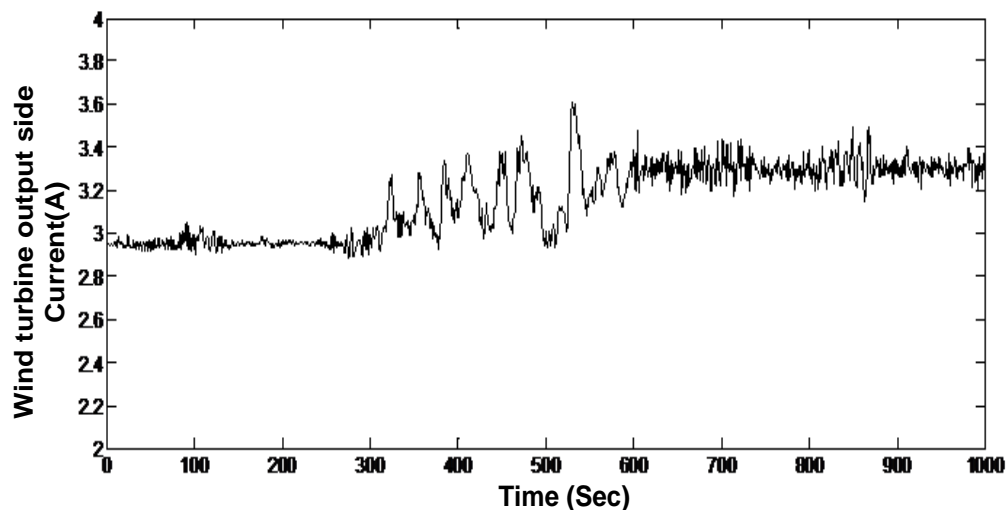


Figure 6.9. RMS Current Measured at the Output of the Wind Turbine

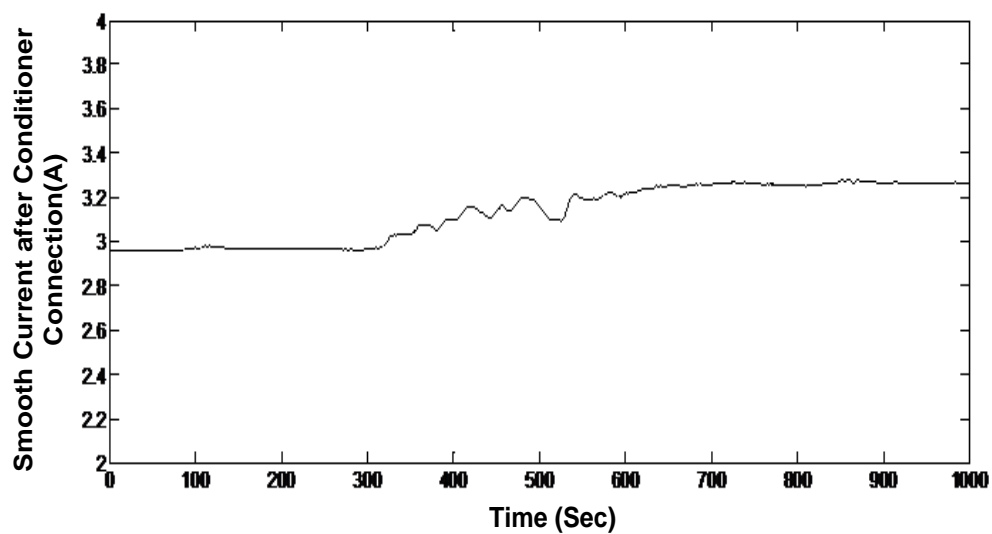


Figure 6.10. Measured RMS Current after connecting the Conditioner

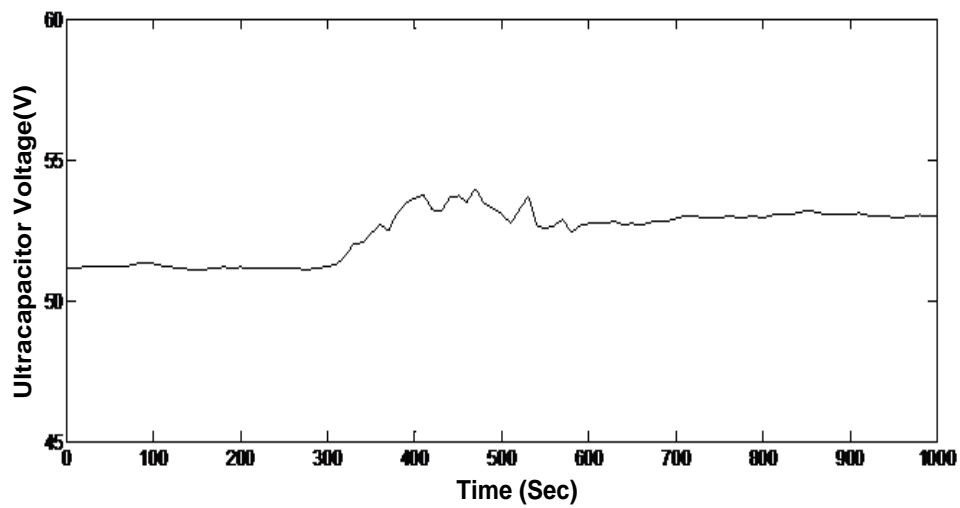


Figure 6.11. Ultracapacitor RMS Voltage

7. CONCLUSION AND FUTURE WORK

In this thesis, the design of a power conditioner and control for smoothing the wind turbine output power with the ultracapacitor is presented. The simulation results show that the proposed conditioner has a good performance in smoothing the wind power. The time constant chosen for the low pass filter in the shunt inverter control is good in getting smooth power. The DC-DC converter maintains the voltage of the DC link relatively constant providing the good controllability of the shunt inverter. The ultracapacitor is charged, when the conditioner draws power from the line and it is discharged, when the conditioner injects power into the line. The hardware of the conditioner is constructed and implemented. The conditioner and its control has been validated by connecting to a wind turbine installed at the Missouri University of Science and Technology. The smoothing performance of the conditioner is matched with the simulation results.

APPENDIX

LIST OF THE COMPONENTS

Line Number	Product Description	Manufacturer and Part Number	Quantity	Price (\$)
1	Prototyping board	VECTOR ELECTRONICS AND TECHNOLOGY – 8016	3	60.99
2	48 V Module Ultracapacitor	Maxwell's Technology - BMOD0165 P048	2	3252.00
3	High Current Power Inductor	West Coast Magnetics - 306-16	1	156.00
4	Microcontroller development board	Microchip - DV164037	1	249.00
5	Voltage Transducer	LEM - LV 25-P	4	210.68
6	Current Transducer	F.W. Bell CLN-50	3	111.54
7	Capacitor ALUM Electrolyte 2000UF, 450V,	VISHAY SPRAGUE - 36DX202F450DF2A	1	64.12
8	IC, QUAD VOLTAGE LEVEL SHIFTER, DIP-16	TEXAS INSTRUMENTS - CD40109BE	2	7.7
9	Optocoupler Gate Driver	Avago Technologies - ACNW3190-000E	6	22.2
10	Dc Power Supply	TP-75C	2	119.68
11	DC-DC Converter	Traco Power - TMA 1515D	6	33.48

12	IGBT Module	SEMIKRON - SK 30 GBB 066 T	1	59.43
13	CAPACITOR PP FILM 600UF, 800V, SCREW	CORNELL DUBILIER - 947C601K801CCMS	1	142.42
14	Digital Signal Controller	Texas Instruments - TMDSDOCK28335	1	102.8
15	LF347 Quad Operational Amplifier	National Semiconductor	4	10.08
16	3-Terminal Adjustable Regulator	National Semiconductor – LM317	4	8.96

BIBLIOGRAPHY

- [1] P. F. Ribeiro, B. K. Johnson, M. L. Crow, A. Arsoy, and Y. Liu, "Energy Storage Systems for Advanced Power Applications," *Proceedings of the IEEE*, vol. 89, no.12, pp.1744-1756, Dec. 2001.
- [2] Ming-Shun Lu, Chung-Liang Chang, Wei-Jen Lee, and Li Wang, "Combining the Wind Power Generation System With Energy Storage Equipment," *IEEE Trans. Industry Appl.*, vol. 45, no. 6, Nov-Dec. 2009.
- [3] Chih-Chiang Hua and Chia-Cheng Tu, "Design and implementation of power converters for wind generator," in *IEEE Industrial Electronics and Applications Conf.*, pp.3372-3377, May 2009.
- [4] M.S.A. Dahidah, N. Mariun, S. Mahmud and N. Khan, "Single phase active power filter for harmonic mitigation in distribution power lines," in *Proc. 2003 IEEE Power Engineering Conf.*, pp. 359- 362.
- [5] Yuanjie Rong, Chunwen Li, Honghai Tang, and Xuesheng Zheng, "Output Feedback Control of Single-Phase UPQC Based on a Novel Model," *IEEE Trans. Power Delivery*, vol. 24, no. 3, July 2009.
- [6] H. Fujita, and H. Akagi, "The unified power quality conditioner: the integration of series and shunt-active filters," *IEEE Trans. Power Electronics*, vol. 13, no. 2, pp.315-322, Mar. 1998.
- [7] A. Kazemi, M. Sarlak, M. Barkhordary, "An Adaptive Noise Canceling Method for Single-Phase Unified Power Quality Conditioner," *IEEE Industrial Electronics and Applications conf.*, May 2006.
- [8] Woonki Na and Bei Gou, "Analysis and control of bidirectional DC/DC converter for PEM fuel cell applications," in *IEEE Power and Energy Society General Meeting*, July 2008.
- [9] Lisheng Shi and M. L. Crow, "Comparison of ultracapacitor electric circuit models," in *IEEE PES General Meeting – July 2008*.
- [10] Bo Chen, Yimin Gao, M. Ehsani and J.M. Miller, "Design and control of a ultracapacitor boosted hybrid fuel cell vehicle," in *Proc. 2009 IEEE Vehicle Power and Propulsion Conf.*, pp.696-703.
- [11] A. S. Samosir and A. Yatim, "Dynamic evolution control of bidirectional DC-DC converter for interfacing ultracapacitor energy storage to Fuel Cell Electric Vehicle system," *Power Engineering Conf*, Dec. 2008.

- [12] R. W. Erickson, and D. Maksimovic, "Fundamentals of power electronics," 2nd ed., New York: Kluwer Academic Publishers, 2000.
- [13] P. T. Krien, "Elements of power electronics," New York: Oxford University Press, 1998.
- [14] H. Akagi, "New trends in active filters for power conditioning," *IEEE Trans. Industry Applications*, vol.32, no.6, Nov/Dec. 1996.
- [15] T. Kai and A. Tanaka, "A new smooth scheme for power fluctuation using inverter of wind power generation with doubly fed induction generator," in *IEEE Electrical Machines and Systems International Conf.*, pp.2390-2395, Oct. 2008.

VITA

Murali Bottu was born on June 9, 1988 in Kanipakam, Andhrapradesh, India. He completed his Bachelor of Technology (B.Tech) in Electrical and Electronics Engineering from Pondicherry Engineering College, Pudhucherry, India in May 2009. He started his Master of Science program in Electrical Engineering at Missouri University of Science and Technology in August 2009 and will receive his Master's degree in Electrical Engineering from Missouri University of Science and Technology in May 2011. His main research interest is Power Electronic Applications to Power Systems.